NEURAL NETWORK-BASED PREDICTION OF MODIFIED CFRP COMPOSITES USED IN AEROSPACE APPLICATION

A PROJECT REPORT

submitted by

MOHAMMED SANAL B

Reg. No: TKM21MECI09

to

the APJ Abdul Kalam Technological University
in partial fulfillment of the requirements for the award of the Degree
of
Master of Technology

in

Mechanical Engineering

Specialization*: Computer Integrated Manufacturing*

Department of Mechanical Engineering

THANGAL KUNJU MUSALIAR COLLEGE OF ENGINEERING

KOLLAM

JULY 2023

DECLARATION

I Mohammed Sanal B, hereby declare that the project report titled "**Neural Network Based Prediction of Modified CFRP Composites used in AeroSpace Application**", submitted for partial fulfillment of the requirements for the award of the degree of Master of Technology of the APJ Abdul Kalam Technological University, Kerala is a bonafide work done by me under supervision of **Dr.Reby Roy K E.** This submission represents my ideas in my own words and where ideas or words of others have been included, I have adequately and accurately cited and referenced the original sources. I also declare that I have adhered to the ethics of academic honesty and integrity and have not misrepresented or fabricated any data or idea or fact or source in my submission. I understand that any violation of the above will be a cause for disciplinary action by the institute and/or the University and can also evoke penal action from the sources which have thus not been properly cited or from whom proper permissionhas not been obtained. This report has not been previously formed the basis for the award of any degree, diploma, or similar title of any other University.

Mohammed Sanal B
Register No: TKM21MECI09 of the year 2021-23
July 2023

12/07/2023

DEPARTMENT OF MECHANICAL ENGINEERING
TKM COLLEGE OF ENGINEERING, KOLLAM

CERTIFICATE

This is to certify that the report entitled **"NEURAL NETWORK BASED PREDICTION OF MODIFIED CFRP COMPOSITES USED IN AEROSPACE APPLICATION"** submitted by **Mohammed Sanal B, TKM21MECI09,** to the APJ Abdul Kalam Technological University in partial fulfillment of the requirements for the award of the Degree of Master of Technology in Computer Integrated Manufacturing is a bonafide record of the project work carried out by him under my guidance and supervision. This report in any form has not been submitted to any other University or Institute for any purpose.

Internal Supervisor:

12/7/23

Dr. Reby Roy K E
Professor
Department of Mechanical Engineering
T K M C E, Kollam

PG Coordinator:

12/7/23

Prof. Kannan S
Assistant Professor,
Department of Mechanical Engineering
T K M C E, Kollam

Head of the Department:

Dr. Dileep P.N
Professor & Head,
Department of Mechanical Engineering.
T K M C E, Kollam

CamScanner

ACKNOWLEDGEMENT

I take this opportunity to express my deep sense of gratitude and sincere thanks to all who helped me to complete the project successfully.

I am greatly thankful to Dr. T.A. Shahul Hameed, Principal, TKM College of Engineering, and Dr. Dileep P.N., Head of the Department, Department of Mechanical Engineering, for providing all required resources for the successful completion of my project.

I am deeply indebted to my guide Dr. K.E. Reby Roy, Professor, Department of Mechanical Engineering for his excellent guidance, positive criticism, and valuable comments.

My heartfelt gratitude to Prof. Kannan S., PG coordinator, Department of Mechanical Engineering, and Prof. Faizal N.S., Assistant Professor, Department of Mechanical Engineering for their valuable suggestions and guidance in the preparation of the project presentation and report.

I am highly thankful to Mr. Manu M, Research Scholar (Ph.D.), and Aravind J,Research Scholar (Ph.D.), Department of Mechanical Engineering for their great support and guidance in the successful completion of this project.

I also express my thanks to the teaching and non-teaching staff of T.K.M. College of Engineering who have supported us in the successful completion of our project.

I will be failing in duty if I do not acknowledge with thanks to the authors of the references and other literature referred to this project.

Finally, I thank my parents, friends, and near and dear ones who directly and indirectly contributed to the successful completion of my project.

Place:KOLLAM

Mohammed Sanal B

July 2023

Abstract

CFRPs, or carbon fiber reinforced polymers, are renowned for having superior wear characteristics. In this study, we compared the wear properties of polycarbonate (PC)/acrylonitrile butadiene styrene (ABS) modified di-glycidyl ether of bisphenol A (DGEBA) based CFRPs with electrophoretically deposited (EPD) carbon fibers. We studied the wear rate (WR) and coefficient of friction (COF) of EPD-modified CF with flexible silanized graphene oxide (SGO) bonds using pin-on-disk experiments. The findings showed significant decreases in COF and WR of 25% and 34%, respectively.

Additionally, the behaviour of the CFRP system with PC/ABS varied depending on the blend ratios. The COF and WR of blends such 70/30, 50/50, and 30/70 showed varied tendencies, however, 10/90 and 90/10 showed consistent decremental patterns, with 90/10 achieving maximum reductions of 19% and 37.9%, respectively. We also looked at how applied load and sliding speed affected wear severity, which changed the wear mechanism from abrasion to delamination. Two testing scenarios were used in the study: room temperature (RT) and cryo-treated (CT).

The sample composition was found to be the most important parameter in terms of volume loss using analysis of variance (ANOVA). A Taguchi analysis was also carried out to optimize the parameters and provide the desired result. We used three predictive models to forecast wear behaviour: the Levenberg-Marquardt algorithm, Artificial Neural Network, and linear regression. The Levenberg-Marquardt algorithm showed the best performance based on mean squared error (MSE) loss, with 2.7% MSE for RT and 2.15% MSE for CT, demonstrating its potential for precise wear behaviour prediction in CFRP composites.

The Levenberg-Marquardt algorithm has a lot of potential for forecasting how CFRP composites will wear. This discovery aids in the comprehension and improvement of CFRP materials for a range of applications needing dependable wear performance.

keywords – Carbon Fiber Reinforced Polymer(CFRP), Poly Carbonate PC/ Acrylonitrile Butadiene Styrene ABS, Silanized graphene oxide (SGO), Analysis of Variance (ANOVA), Mean Square Error(MSE), Linear Regression(LR), Artificial Neural Network (ANN).

Contents

List of Figures

List of Tables

ABBREVIATIONS

AI	Artificial Intelligence
ML	Machine Learning
CFRP	Carbon Fiber Reinforced Polymer
CF	Carbon Fiber
RT	Room Temperature
CT	Cryo-Treated
S.G.O	Silanized Graphene Oxide
C.O.F	Coefficient of Friction
WR	Wear Rate
ANOVA	Analysis of Variance
ETA	Effect Size Measure
LR	Linear Regression
ANN	Artificial Neural Network
ABS	Acrylonitrile Butadiene Styrene
PC	Polycarbonate
DGEBA	Diglycidyl Ether of Bisphenol A
P-Value	Probability Value
SN	Signal-Noise
EPD	Electrophoretic Deposition
NaN	Not a Number

Chapter 1

INTRODUCTION

In the modern era, composite materials are defined as two or more separate materials that have been joined in a way that causes them to exhibit characteristics that differ from those of their parent materials. When such materials are mixed, they show characteristics that are better than those of their constituent components. When this substance is combined with a polymer matrix, the strength, stiffness, and toughness of the resulting composite material can be improved. As a result, these materials have a wide range of uses in the construction, automotive, and aerospace industries.

1.1 Carbon Fiber

Carbon fibre is created from a chain of carbon atoms joined together by chemical bonds. The fibres made from carbon typically have a diameter between 5 and 10 micrometres. The fibres are extremely stiff, strong, and light, and they are used in a variety of processes to create high-quality structural materials. Carbon fibres are outstanding for their high stiffness, exceptional tensile strength, low weight, excellent chemical resistance, high endurance to high temperatures, and limited thermal expansion. Since carbon fibre is around five times lighter than steel, which is much denser, carbon fibre is approximately five times stronger than steel in this regard. Due to its unmatched strength-to-weight ratio, carbon fibre is the material of choice for applications (aerospace, sporting goods, etc.) where minimising weight is important. As these carbon fibre's constituent strands are even smaller than human hair, they can be used to manufacture lightweight clothing [5]. Materials with certain weaving patterns, such plain or twill weaves, or cloth can all be used to obtain carbon fibre reinforcement. This guarantees a productive and effective manufacturing process.

Since these carbon fibres can be utilised to manufacture lightweight clothing because their individual strands are even smaller than human hair. Materials with certain weaving patterns, like plain or twill weaves, or cloth, can all be used to create carbon fibre reinforcement. This guarantees a productive and effective manufacturing process.

Polyacrylonitrile (PAN), which makes up the majority of the precursor, often referred to as the raw material for the synthesis of carbon fibres, accounts for about 90% of the fibres made. Petroleum pitch or rayon make up the final 10% [5]

Since these carbon fibres can be utilised to manufacture lightweight clothing because their individual strands are even smaller than human hair. Materials with certain weaving patterns, like plain or twill weaves, or cloth, can all be used to create carbon fibre reinforcement. This guarantees a productive and effective manufacturing process.

In contrast to the 1960s, when their initial iteration was too fragile and weak to be used in any industry, continuous innovation has led to its current status as a material with many uses, from the automotive and aerospace industries to the military and sports, among others. Their use has increased dramatically since they are both substantially stronger than steel and significantly lighter than steel, which allows them to sustain stress even in high-speed applications while still displaying the properties of being low-weight.

1.2 Manufacturing of Carbon Fiber:

PAN (polyacrylonitrile), '[12], which makes up about 90% of the precursors, is one of the primary components of carbon fibre. Rayon or petroleum pitch commonly make up the remaining 10%. These precursors are selected for their organic makeup because they have long chains of chemically linked organic molecules. Carbon fibre's creation and attributes are greatly influenced by this composition, which also gives it its desirable properties including high strength, lightweight, and outstanding thermal and electrical conductivity.

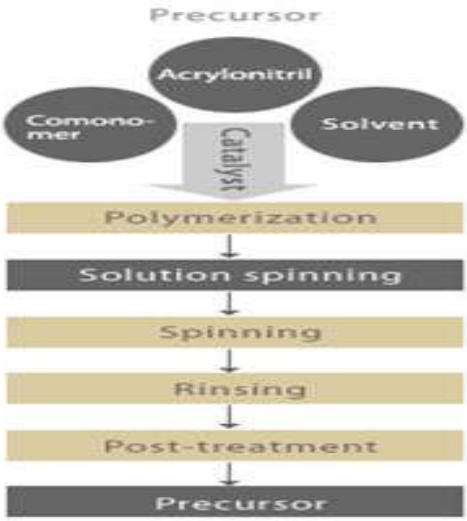

Figure 1.1: PAN Process

‘[5]

1.2.1 spinning

A standard suspension or solution polymerization technique for PAN Plastic s created when acrylonitrile plastic powder is combined with another plastic, such as methyl methacrylate, and then reacts with a catalyst. After being spun into fibres, the plastic is combined with specific chemicals and forced through tiny jets where it coagulates and solidifies into fibres. Thin fibres that have undergone processing are then cleaned and stretched to the requisite diameter. Stabilising comes next after these processes. Prior to carbonization, the fibres must first undergo stabilisation in order to change their linear atomic bonding to a more thermally stable ladder bonding. This technique involves heating airborne fibres to a temperature of roughly 200–300 °C for a duration of 30–120 minutes. As a result, oxygen molecules are attracted to the fibres from there and are then rearranged through their bonding structure. The process of carbonising comes next after stabilising effectively.

1.2.2 Stabilizing:

Prior to carbonization, the fibres must first undergo stabilisation in order to change their linear atomic bonding to a more thermally stable ladder bonding. This technique involves heating airborne fibres to a temperature of roughly 200–300 °C for a

duration of 30–120 minutes. As a result, oxygen molecules are attracted to the fibres from there and are then rearranged through their bonding structure. The process of carbonising comes next after stabilising effectively.

1.2.3 Carbonizing

The carbon fibres are first heated to a temperature of around (1000-3000 degrees Celsius) in a furnace that is oxygen-free during the carbonising process. cutting off oxygen to stop any burning of the fibres. While the carbon atoms that are already present establish tighter bonds that are more or less aligned parallel with the axis of the fibre, the non-carbon atoms are lost or expelled during heating.

1.3 Carbon Fiber's Composition:

A Carbon Fibre is made of carbon atoms arranged in a regular crystalline structure. The carbon atoms are bonded together in a strong, covalent bonding structure, forming a hexagonal lattice known as graphene following a regular hexagonal shape. Depending upon the way carbon fiber is being manufactured, they may either be turbo static, graphitic or a hybrid structure. In a typical structure of Carbon fibre, Within carbon fiber, the carbon atoms are aligned in a parallel and orderly manner along the length of the fiber, resulting in a crystalline structure that augments the mechanical properties of the material. These individual carbon filaments are bundled together, forming larger structures known as fiber bundles. These bundles consist of numerous tightly packed filaments, often numbering in the thousands.

To optimize the strength and stiffness of the material in desired directions, the carbon fibers within carbon fiber composites are usually arranged in specific orientations. Engineers can manipulate the fiber orientation during the manufacturing process to tailor the properties of carbon fiber for specific applications. The carbon fibers within carbon fiber are bound together by a polymer matrix, typically composed of epoxy or a similar material. This matrix envelops and safeguards the carbon fibers, imparting impact resistance and enhancing the overall structural integrity of

the composite material.

1.4 Carbon fibre characteristics:

High modulus and specific tensile strength are two of carbon fiber's desirable properties (these properties are improved by the presence of graphite crystallites). These characteristics demonstrate that carbon fibre can serve as a replacement to many commonly used materials or chemicals.

Carbon fibres with higher modulus and strength are used as reinforcement in polymeric composites, whilst fibres with lower modulus and strength characteristics are used as fillers. Excellent electrical and thermal conductivities are also demonstrated by carbon fibres. The increased fatigue resistance of using these fibres in composite materials is a significant benefit. Carbon fibres do not exhibit stress rupture, but rather complete elastic recovery upon unloading, in contrast to aramid or glass fibres. Since the graphite structure and the graphene layers are responsible for the electrical conductivity of carbon fibres and since the layers are semiconducting between them, carbon fibres have anisotropic electrical characteristics . These fibres exhibit chemical inertness since they are normally unaffected by air, humidity, weak acids, alkalis, and solvents. At high temperatures, they are vulnerable to oxidation, albeit.

The low shock resistance of carbon fibres as a result of their high fragility and rigidity, as well as their vulnerability to chemical attack in the presence of oxidising substances and oxygen at temperatures above 400°C, are some downsides. The extensive application of carbon fibres is severely constrained by cost. The cost of carbon fibres can typically be justified when significant weight savings are realised, especially in aerospace applications, or when high-temperature performance, corrosion resistance, improved fatigue strength, or long-term strength retention are essential for the intended use '[19]. Since their high price has so far limited their wide range of commercial uses, the aerospace sector, where weight reduction is more important than cost, is where they are most commonly used.

1.5 Carbon Fiber Pattern:

Carbon fibre is structured in a variety of patterns or weaves depending on the necessary mechanical properties and capabilities.

1.5.1 Plain Weave:

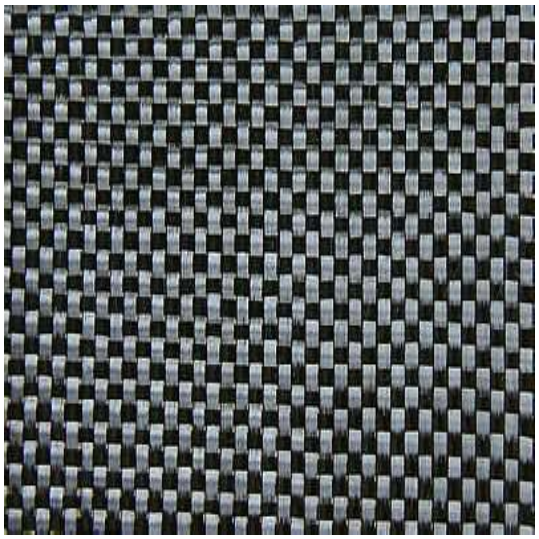

Figure 1.2: Plain Weave,courtesy:(estcarbon)

A carbon fibre sheet that has been woven in a plain weave pattern has an even appearance that resembles a little checkerboard pattern. They are interwoven or twisted together by arranging the weaves in an over/under pattern. The explanation for this is that the interlaces' close closeness helps explain the plain weave's pronounced stability. The ability of a fabric to maintain its weave angle and fibre orientation is referred to as fabric stability. Due to its strong stability, the plain weave is not good for layups with delicate shapes since it may lack the desired pliability displayed by other weave patterns. This is the arrangement's main drawback. In general, applications involving flat sheets, tubes, and 2D curves work best with plain weave materials. The tolerance damage is also significantly decreased in woven fabric.

1.5.2 Twill weave

Twill weave serves as a transitional weave between plain weave and satin weaves. It offers superior fabric stability than a harness satin weave and offers good flexi-

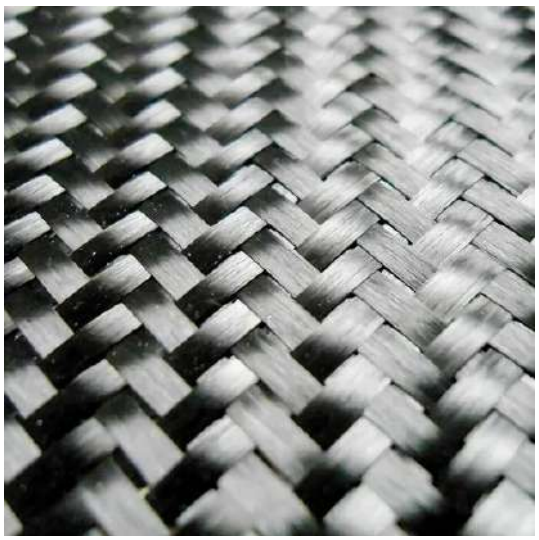

Figure 1.3: Twill weave,courtesy:(estcarbon)

bility while allowing it to adjust to complex curves. If you trace a tow strand in a twill weave, it will pass over a certain number of nearby tows before going under the same amount of tows. The "twill line," which is produced by this over/under pattern, is a recognizable diagonal arrowhead appearance. Twill weave has wider tow interface spacing than plain weave, which causes fewer crimps and less possible stress concentrations.

1.5.3 Harness Satin Carbon Fiber Pattern

Figure 1.4: Harness Satin Carbon Fiber Pattern,courtesy:(estcarbon)

In such a construction, the warp yarns serve to link the weft floats whereas the weft yarns may be seen predominately in the fabric face layer. These structures

become more distinct the further apart they are from one another. When more yarns are intertwined, the resulting fibre structures are stringy, however when there is less interlacing, pliability and resistance to wrinkling become desired properties for the resulting structures.

1.5.4 Unidirectional Carbon Fiber pattern

Figure 1.5: UniDirection Carbon Fiber Pattern,courtesy:(estcarbon)

Such fibre orientations cause the carbon fibres to travel in a single, parallel direction. They are utilised in applications where durability is desired since they are stronger than alternative fibre orientations, such as woven fibre. The plies can also be orientated with a larger percentage along one of the axes, or they can be put out in numerous directions to obtain balanced mechanical qualities.

1.6 Epoxy resin

These monomers contain at least two epoxide groups and are used to create a type of high performance polymers. Their exceptional strength, hardness, stickiness, and chemical resistance are what set them apart. Epoxy resins are utilised in a wide range of products, such as electrical parts, adhesives, coatings, and composites.

1.6.1 Properties of Epoxy resin

- superior toughness and strength.

- fantastic adherence to a variety of substrates.
- Excellent Thermal Stability.
- excellent chemical resistance.
- Less Characteristics of Reduction or Shrinkage.
- Low electrical characteristics

1.6.2 Types of Epoxy Resins:

1. Bisphenol A-based epoxy resins:

   Epoxy resins made with a base of bisphenol A are the most popular kind. They are renowned for their extreme toughness, chemical resistance, and strength. Additionally, these materials have good weather resistance, superior electrical insulation, etc.

2. cycloaliphatic epoxy resins:

   Being more heat- and chemical-resistant than epoxy resins based on bisphenol A. They have a molecular structure like a ring and have low viscosity, low molecular weight, UV and moisture resistance, superior color, and a glossier finish, among other qualities. If cost factors are taken into account, they are also more expensive, which makes it less desirable to use.

3. Epoxy esters:

   These resins are derived from epoxidized oils. They are more flexible and impact-resistant than bisphenol A-based epoxy resins.Likewise, such materials can also act as corrosion inhibitors.

1.7 Carbon Fiber Reinforced Polymer:

CFRP ‘[23], short for Carbon Fiber Reinforced Polymer, is a composite material that combines the flexibility and versatility of a polymer matrix with the strength and stiffness of carbon fibers. Its exceptional mechanical properties, lightweight nature, and resistance to corrosion make it highly sought-after across various industries.This

is done as partially-impregnated composites exhibited better tribological properties under severe conditions‘[29].

1.7.1 Properties of CFRP:

- CFRP boasts an impressive strength-to-weight ratio, providing remarkable tensile and compressive strength alongside stiffness.
- The lightweight nature of carbon fibers contributes to the overall reduction in the composite structure's weight.
- Excellent Thermal Stability.
- excellent chemical resistance.
- Less Characteristics of Reduction or Shrinkage.
- Low electrical characteristics

1.8 Statistical Tools for Optimization and Analysis in CFRP Manufacturing: Taguchi Methods and ANOVA

In CFRP (Carbon Fiber Reinforced Polymer) research, Taguchi methods and analysis of variance (ANOVA) can be used to analyse and optimise manufacturing processes and performance ‘[25]

1.8.1 Taguchi Method

Developed by Genichi Taguchi, Taguchi methods are statistical techniques for robust design and optimization. They seek to reduce the variation in product performance induced by various sources of variation, such as process parameters and material properties. Typically, Taguchi methods employ design of experiments (DOE), in which a series of experiments are conducted with varying parameter settings to determine their effects on the response variable(s). This enables the identification of key factors and their optimal configurations for enhancing the quality or performance of CFRP components ‘[22].

1.8.2 Analysis of Variance(ANOVA)

ANOVA is a statistical technique used to determine the significance of different factors or treatments by analysing the variance in a dataset. ANOVA can be used to analyse the effects of various process parameters, material compositions, and other factors on the mechanical properties of CFRP materials, such as tensile strength and flexural modulus. ANOVA aids in identifying the influential factors on the response variable and quantifying their contributions to the overall variance‘[7].

Hypotheses are evaluated using ANOVA (Analysis of Variance) to determine the significance of factors or treatments on the response variables of interest. ANOVA hypotheses are typically expressed as follows:

Null Hypothesis (H0): There is no significant difference between the means of the groups or treatments. Alternative Hypothesis (HA): There is a significant difference between the means of the groups or treatments. In this case, the null hypothesis would state that the mean values of the output parameters (e.g., tensile strength, flexural modulus) are the same across different levels or combinations of input parameters (e.g., process parameters like RPM, load,sliding distance, material compositions). The alternative hypothesis, on the other hand, suggests that there is a significant difference in the means of the output parameters among the different levels or combinations of input parameters.

To determine whether to accept or reject the null hypothesis, ANOVA calculates the F-statistic and compares it to a critical value. If the calculated F-statistic is larger than the critical value, it indicates that there is a significant difference between at least two groups or treatments, and the null hypothesis can be rejected. On the other hand, if the calculated F-statistic is smaller than the critical value, it suggests that there is no significant difference among the groups or treatments, and the null hypothesis cannot be rejected.By conducting ANOVA, researchers can identify the influential factors and determine their contributions to the variability in the output parameters. This information helps in optimizing the manufacturing process and making informed decisions to improve the quality and performance of CFRP composites.

1.9 Artificial Intelligence and Machine Learning:

1.9.1 Artficial Intelligence

Nowadays, Artificial intelligence (AI) is a buzzword and a powerful tool that can be used to improve the design, performance, and efficiency of mechanical systems.

In the field of manufacturing‘[1], they have considerable benefits, which include::

- Design optimization: AI can be used to explore vast design spaces and identify the most beneficial configurations, materials, and parameters. This can lead to improved performance, reduced weight, or increased efficiency.
- Predictive maintenance: AI can be used to analyze sensor data and historical performance records to predict mechanical failures and maintenance requirements. This can help prevent costly breakdowns by enabling timely maintenance interventions.
- Robotics and automation: AI is playing a crucial role in the development of robotic systems that can learn from experience, adapt to changing environments, and perform complex tasks with minimal human intervention.
- Quality control: AI-based image processing and machine vision systems can be used to inspect manufactured components for defects, deviations, or nonconformities. This helps to ensure high-quality production and reduces the occurrence of human errors during the inspection process.moreover, in the tough environment conditions where manufacturing is difficult Artificial Intelligence can play a divisive role in solving problems.
- Energy efficiency: AI can be used to optimize energy consumption in mechanical systems. By analyzing real-time operational data, AI algorithms can dynamically adjust parameters to minimize energy waste, improve system efficiency, and reduce environmental impact.
- Structural analysis and simulation: AI can be used to enhance the accuracy and speed of structural analysis and simulation. Machine learning algorithms can learn from extensive datasets of simulation results, generating surrogate

models that reduce computational time while maintaining acceptable accuracy levels.

1.9.2 Machine Learning

‘[1]With the meteoric rise in generation of data, real time changes need to be made. Therefore, machine learning is being used in every domain. In research, machine learning has attracted a lot of attention and interest. The primary reason why such a data-driven approach has now taken hold is, for example, with the data generated, like the coefficient of friction, through experimental or simulation, we can understand and predict the coefficient of friction in various applications, thus giving valuable insights, saving time and resources in the process.

1.9.2.1 1.8.2.1 Linear Regression:

Linear regression is a type of supervised learning technique within the discipline of machine learning. It is used to represent the association between a dependent variable (output) and one or more independent variables (input). Linear regression is frequently employed in numerical analysis and prediction assignments where the objective is to predict a continuous output variable given the values of input variables.

In the context of predicting wear, for instance, linear regression can be applied by considering input variables such as load, RPM, and others, and the output variable as wear. By training a linear regression model on a dataset containing known input-output pairs, the model is able to learn the underlying patterns and relationships between the input parameters and the wear, thereby enabling predictions for new input values.

Therefore, linear regression is a useful instrument for analyzing numerical data and predicting continuous variables, making it appropriate for applications such as parameter-based wear prediction.

1.9.3 Artificial Neural Network (ANN)

Artificial Neural Networks (ANNs)‘[1]], are computational models inspired by the structure and functioning of the human brain. In recent trends and development this ANN algorithm have gained wide popularity in various fields, including the

analysis and prediction of CFRP (Carbon Fiber Reinforced Polymer) composites.

An ANN consists of interconnected nodes, known as artificial neurons that are organized in layers. They typically include an input layer, one or more hidden layers, and an output layer. Each neuron receives inputs, applies a mathematical transformation to them, and passes the transformed values to the next layer.

In the context of CFRP composites, ANNs can be trained to learn complex relationships between input variables (e.g., sample compositions, load, RPM) and output variables (e.g., coefficients of friction, wear rate). The training process involves presenting the network with a set of input-output pairs and adjusting the weights and biases of the neurons to minimize the prediction errors.

In the analysis of CFRP composites ANN offers several advantages. They can accurately capture nonlinear relationships, while handling large amounts of data. ANNs can also learn from examples and generalize well to unseen data, enabling predictions and optimizations for different composite configurations.

To build an ANN for CFRP composites, data collection and preprocessing are crucial. Relevant input variables and corresponding output variables are identified, and a suitable dataset is prepared for training and testing. The dataset is typically divided into training and validation subsets to evaluate the model's performance.

The architecture of the ANN, including the number of layers, neurons per layer, and activation functions, is determined based on the complexity of the problem and available data. Hyperparameters such as learning rate, batch size, and regularization techniques are adjusted to optimize the training process.

Once the ANN is trained, it can be used to make predictions for new input data, providing insights into the behavior and performance of CFRP composites. The ANN can help researchers and engineers optimize composite designs, understand the impact of different parameters, and improve the overall performance and durability of CFRP structures.

Overall, ANNs offer a powerful tool for analyzing and predicting the behavior of CFRP composites, enabling researchers to make informed decisions and advancements in aerospace, automotive, and other industries where CFRP materials are extensively used.

In the CFRP application, the models which analyses the relationship between four input parameters—time series, load, rpm, and sample composition—and two output parameters—C.O.F and wear rate being developed. The models investigates how

various input factors affect CFRP material C.O.F and wear. We can optimise modified CFRP performance in diverse applications by using this model to understand its tribological behaviour.

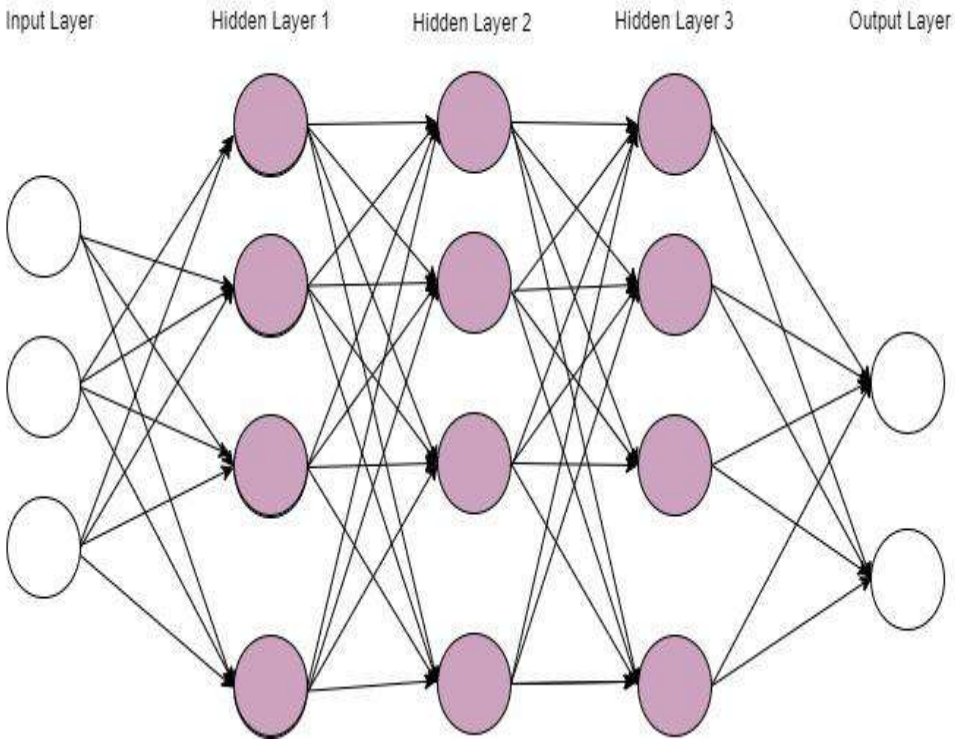

Figure 1.6: Artificial Neural Network

1.9.4 Levenberg-Marquardt algorithm:

The Levenberg-Marquardt algorithm '[9], is a commonly used optimisation technique for solving nonlinear least squares problems. It incorporates the strengths of the Gauss-Newton method and the steepest descent method.

The algorithm seeks to determine the optimal values for a model's parameters by iteratively modifying them using the Jacobian matrix and the Hessian matrix. The Jacobian matrix represents the partial derivatives of the model's equations with regard to the parameters, whereas the Hessian matrix represents the partial derivatives of the second order.

The Levenberg-Marquardt algorithm effectively converges to the optimal solution through the use of the Gauss-Newton method, which is based on linear approximations, and the steepest descent method, which is based on gradient descent. It modifies the update step size in accordance with a damping factor, allowing for more stable convergence.

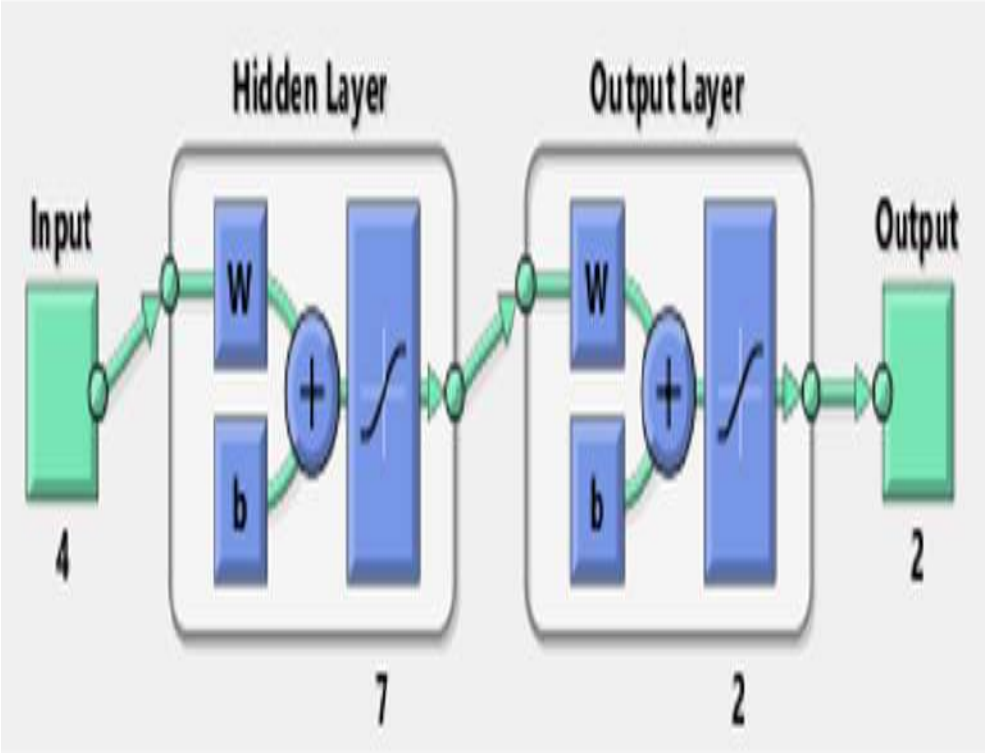

Figure 1.7: Artificial Neural Network Deployed

The Levenberg-Marquardt algorithm is a potent optimisation method that can effectively solve nonlinear least squares problems by iteratively updating the parameters with the Jacobian and Hessian matrices. Thus, it is appropriate for use in the CFRP application for accurately predicting the intricate relationship established within the system.

Chapter 2

LITERATURE REVIEW

Santhosh Kumar(2022) [13] In this paper Initially, glass fibre reinforced polymer (GFRP) composites and GFRP composites containing 0.5 wt% and 1 wt% graphene nano-platelets (GNPs) by manual lay-up method are manufactured. Then, tribological testing is conducted, and an artificial neural network technique is used to analyse the data. On this basis, the Pin on Dis Tribo-tester is a reliable instrument for determining the tribological properties of composite samples. In addition, he has investigated how the Artificial Neural Network (ANN) technique can be used to predict the wear and coefficient of friction (COF) for GFRP composites and GFRP composites containing graphene nano-platelets (GNPs).

XIANBO XU(2019) [30] The paper determines the elastic modulus of carbon fiber-reinforced polymer over a wide range of temperature and strain rates by devising an artificial neural network method. The paper demonstrates how precise results can be obtained using ANN regardless of the material's composition and quality. Thus, the approach attained an error of less than 7.3%, indicating that the elastic modulus of any material can be accurately predicted. Regarding fibre orientation, their method also anticipated the behaviour of anisotropic material at a variety of orientations.

Wei Shao(2023) [26] The paper highlighted the three phases of deflection and propagation in CFRP materials: elastic deformation, crack propagation, and failure. They also examined the material's rigidity reduction factor, which decreases more slowly with an increase in CFRP reinforcement. In other words, as the proportion of CFRP increases, the decrease in composite piles' bending resistance becomes less pronounced. Additionally, the paper examined the effect of horizontal displacement on CFRP composites, concluding that as the proportion of CFRP reinforcement

increases, the composites become susceptible to horizontal displacement.

Prabhath Kumar(2020) [25] Through this paper, the effect of friction, wear behaviour of CFRP composites based on Taguchi design on the process parameter Load, sliding speed, and sliding distance has been investigated. According to the results of their experiment, load and sliding speed are significant parameters affecting the output COF and specific wear rate. The relationship between sliding distance and specific wear rate is weaker.In addition, an ANOVA test is conducted to determine the significance of each process parameter in relation to the test parameter. Thus, they realised that normal load has a more significant influence on the COF of CFRP composites and ranked it first, followed by sliding speed and sliding distance.Normal load and gliding speed have a greater impact on specific wear rate than other parameters.

A. Borjali(2019) [6]The paper presented a data-driven, machine-learning-based method for predicting the polythene degradation rate in Pin-on-Disc (POD) experiments involving prosthetic hip implants. So, by accumulating data from other published polythene wear data, we implemented multiple data-driven models using various machine learning techniques. The paper emphasised the relative contributions of each POD parameter and its effect on the output.In conclusion, the data-driven machine learning model can be used to predict the polyethylene degradation rate in Pin-on-Disc (PoD) experiments in the context of prosthetic hip implants.

Vipin Kumar Tripathi(2019) [27] In this paper, the effect of sliding wear behaviour of a carbon fibre reinforced polymer (CFRP) hybrid nano composite with montmorillonite nanoclay and nanoZnO as additives was investigated. They have also examined the wear resistance of CFRP hybrid nanocomposites using a pin-on-disc machine under varying pressures. In addition, they predicted the effect of the independent variables, wt% nanoZnO, nanoclay, and fibre orientation angle, on the wear rate of CFRP hybrid nanocomposites. Also analysed was the effect of nanoclay and fibre orientation on attrition rate, revealing an increasing trend and mutual interaction.The novel material, i.e., CFRP hybrid nanocomposites with nanoclay and nanoZnO incorporation, can be used in a variety of applications, including carbon-carbon disc brakes, friction clutches, and various components of spacecraft, aeroplanes, and automobile gearboxes.

Hali Ibrahim(2015) [14] The paper then used an artificial neural network to effectively predict the dry sliding behaviour of UHMWPE composites with different

fibres and particles under a variety of operating conditions. This was accomplished by compiling and utilising extensive experimental results taken from a variety of sources. The study discovered that sliding speed and applied load have a greater influence on the volume loss of UHMWPE composites than other input parameters. The proposed NN model and the explicit form of mathematical formulation derived from it demonstrate good accord with test results and can be used to predict the volume loss of UHMWPE composites. In addition, the proposed neural network demonstrated excellent accord with experimental results.

Hiral H(2017) [24] This paper investigated the wear behaviour of cotton fibre reinforced polyester composites with variable graphite filler amounts. Contributions of this paper include how cotton fiber-reinforced polyester composites with variable amounts of graphite fillers are fabricated by hand using a lay-up technique. In addition, they examined the influence of graphite content on the dry sliding wear behaviour of cotton fibre polyester composite (CFPC) using a pin-on-disc machine (POD) test setup.utilising response surface methodology (Box Behnken method) to systematically reduce the quantity of experiments. SEM analysis was also performed in the paper to investigate the degradation mechanism. In a nutshell, their findings on the degradation behaviour of CFPC can be applied to future investigations in this field.

Challa Gangu Naidu(2023) [20] The article highlighted the outstanding properties of carbon fiber-reinforced polymer (CFRP), such as its low weight, high strength, high modulus, and high temperature resistance. In addition, they described the vast array of prospective applications for CFRP composites, which include public safety, aviation, and high-end non-military consumer goods. In the middle of the 1950s, CFRP was first used in the automotive industry, followed by a variety of other industries, such as commercial spares (aircrafts, chartered flights, defence sector spares), underground energy (oil production, gas pipelines), green energy generation (hydrogen fuel, electricity transmission), and the construction field (civil aviation).

M.V. Gordić et al(20017) [10] The journal highlighted an experimental investigation of the Mode of interlaminar fracture of unidirectional carbon fibre and epoxy composites. In a double cantilever beam (DCB) test, the energy release rate GIC of the Mode I delamination strain was evaluated before and after gamma irradiation at various doses. The glass transition temperature (Tg) of the epoxy matrix was determined by means of dynamic mechanical experiments. On the tested coupons,

SEM images of the delamination surfaces were acquired.

Y He et al (2013) [11] Adding thermoplastics to epoxy (YD-128) and carbon fibre reinforcing helped alter the material's various properties, according to the study. For the modification of epoxy, three distinct thermoplastics (PEI, PC, and PBT) were utilised. To reinforce carbon fibre in epoxy laminates, vacuum-assisted resin transfer moulding (VARTM) was used. The modified epoxy contains a maximum of 1.5wt% thermoplastic. In their investigation, they employed a variety of techniques, including impact testing, morphological analysis, thermomechanical analysis, dynamic mechanical analysis, thermogravimetric analysis, and laminate microcracking. At cryogenic temperatures, they discovered that the impact strength of PEI-modified epoxy was 45 percent greater than that of unmodified epoxy. At ambient temperature, the impact resistance of PEI increased by 59%.At cryogenic temperatures, PC and PBT also enhanced the impact strength of the modified epoxy matrix. When evaluated at room temperature, the impact strength increased to 1.5wt% before diminishing.

Zhenhua Zhang(2014) '[31] In this article, the tribological behaviours of carbon fibre reinforced polyetheretherketone (CFR PEEK) moving on silicon carbide ceramic while lubricated with seawater are investigated. The following are the primary inferences that may be made from the outcomes of the experiment: Under conditions of lubrication provided by seawater, the friction pair demonstrates outstanding friction and wear resistance. The critical friction running-in process is significantly impacted by the sliding velocity that is being applied.When the sliding velocity is 1 metre per second and the contact pressure is 1.98 megapascals, the minimal friction coefficient is very close to reaching 0.05. The amount of time necessary for adjustment decreases steadily with an increase in contact pressure; nevertheless, the fluctuation of friction coefficient becomes more severe after the running-in stage has been completed.When the contact pressure is increased, there is a minor drop in the wear rate of CFR PEEK; however, there is no significant change in the amount of mass lost by silicon carbide ceramic.The two most important tribological mechanisms of CFR PEEK are mechanical ploughing and adhesive wear, both of which are caused by surface micro-peaks of silicon carbide ceramic.

H.A. Al-Salihi(2019) [2] Mechanical and wear behaviour of AA7075 aluminium matrix composites were investigated in this paper. The high mechanical properties of 7075 alloy are utilised in a variety of application sectors, including gears, shafts,

and aviation fittings, as he explained. Wear is a significant process that occurs when these elements move between two surfaces. Consequently, material loss due to wear can result in significant industrial process malfunctions.

M.Manu(2022) [17] According to the findings of the study, the indigenous cross-linking density of epoxy can be successfully reduced by adding 3-aminopropyltrimethoxysilane to epoxy. This results in an increase in epoxy's toughness; however, this comes at the expense of epoxy's overall strength. After the completion of more in-depth research, the CFRP that has been created may become a candidate for use in the construction of cryo tank materials. The research also indicates that the crack deflection phenomena was seen, which has the potential to contribute to the dissipation of a significant amount of energy when subjected to impact stresses.

Aravind J(2023) [3] The study came to the conclusion that modifications made in epoxy resin utilising a thermoplastic material, such as polycarbonate (PC) and/or acrylonitrile butadiene styrene (ABS), exhibit high thermal resistance (TR) of 77.1% when compared to unmodified CFRP. These results were taken from the findings of the study. The transmission rate (TR) of modifications that were created utilising conductive mediums such as phosphonium (P), imidazolium (I), or silanized-graphene oxide (SGO) was reduced by 25.7%, 30.5%, and 32.4%, respectively. By the effect of synergistic strategy that makes use of the effect of a variety of conductive and insulative modifiers with diglycidyl ethers of bisphenol A (DGEBA) epoxy resin and/or carbon fibre (CF), we can achieve our goal. In order to get the greatest improvement in the thermal conductivity of CFRP laminates, the I 0.5 modification and the G 1.0 modification are the two modifications that show to be the most successful. Thermogravimetric analysis (TGA) tests demonstrate that I 0.5 and G 1.0 modified CFRP perform better than P 0.5 modified CFRP in thermal conductive applications throughout a temperature range of 100 to 150 degrees Celsius. This was determined by comparing the three types of modified CFRP. In general, across the temperature range of 200 to 250 degrees Celsius, the performance of 90/10 modified CFRP is superior to that of all other modifications and unmodified CFRP. When compared to unmodified CFRP, 90/10 modified CFRP performs wonderfully over a temperature range of 100 to 200°C, with a maximum weight loss percentage of just 2.08%. As a result, it is ideal for applications that require good thermal insulation capabilities and may be used in a wide variety of settings. The synergy effect is the focus of this particular research project.

Wutao Dong(2013) '[8] In this study, the authors investigate how the sliding velocity and load affect the tribological behaviour of PEEK filled with short carbon fiber/PTFE/Graphite as it slides against AISI630 stainless steel with water as the lubricant. According to the findings, the tribological behaviour of the materials is significantly influenced mostly by the sliding velocity. The formation of hydrodynamic lubrication was made easier at higher sliding velocities; however, the quick increase in temperature that accompanied the higher sliding velocities had a negative impact on the water lubrication layer. When the load was 1.66 megapascals and the sliding velocity was between 1.5 and 2 metres per second, adhesive wear became the most important element in the sliding process. When the load that was being applied to the specimens was increased to between 2.49 and 3.32 MPa, the surface of the PEEK began to develop cracks and delamination wear.

Chapter 3

METHODOLOGY

3.1 Sample Preparation:

The carbon fiber is first modified based into various compositions. This is done based on using a) (carbon fiber, EPD coated with SGO) + (DGEBA epoxy), b) (neat carbon fiber) + (PC/ABS melt mixed in DGEBA epoxy). 3) (DGEBA epoxy, Neat Carbon Fiber)

3.1.1 Electrophoretic Deposition (EPD) coating on CFRP composites:

The electrophoretic deposition (EPD) process was utilized in the manufacturing of Carbon Fiber Reinforced Polymer (CFRP) composites, specifically for the coating of graphene-based nanofillers onto carbon fiber surfaces. The EPD process involves the application of an electric field to drive the migration and deposition of charged particles suspended in a liquid medium.

In this case, the graphene nanofillers were first oxidized and then functionalized with silanes. The silanized graphene (SG) suspension was prepared by sonicating the SG with deionized water. The carbon fiber sheets and stainless steel plates were arranged in parallel, serving as the cathode and anode, respectively, within the EPD bath.

During the EPD coating process, a constant voltage of 30 V was applied for 20 minutes. To ensure effective dispersion of the nanofillers and removal of bubbles that could hinder nanoparticle deposition, the EPD process was conducted within a sonicator. As a result, the SG particles were successfully coated onto the carbon fiber surface.

Subsequently, the CFRP laminate was fabricated using the Vacuum Assisted Resin Transfer Molding (VARTM) technique, employing a 2:1 epoxy/hardener ratio. The epoxy/hardener mixture was degassed in a chamber to eliminate air bubbles. The resulting laminates were named as 0.5 SG, 1.0 SG, and 1.5 SG based on the concentration of silanized graphene used in the EPD process.

In summary, the EPD process played a crucial role in the manufacturing of CFRP composites by facilitating the deposition of graphene-based nanofillers onto carbon fiber surfaces. This process enhanced the mechanical and functional properties of the composites by introducing the desired nanofiller coating.

Figure 3.1: EPD Setup process

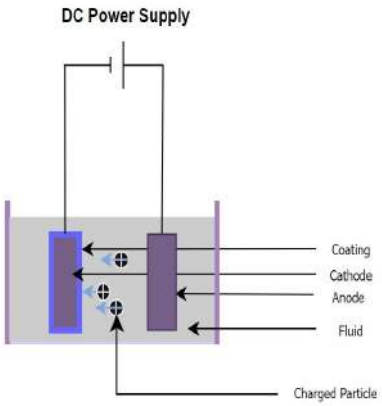

Figure 3.2: EPD Schematic Representation

3.1.2 DGEBA-PC/ABSMelt Mixed composites:

For the manufacture of this sample, DGEBA epoxy resin is first melt mixed with desired thermoplastics compositions of PC and ABS. Melt mixing is done, so as to reduce the chances of void development during curing. Followed by that, degassing is done to remove any trapped bubbles that may have formed due to poor mixing with the hardener.

3.2 Specimen Preparation:

These modified composite specimens and unmodified CFRP were then modified by handlaying the CFRP first and then carrying out VARTM process to achieve effective impregnation of the fiber reinforcement with resin

3.2.1 Layup process for CFRP before VARTM:

During the layup process of CFRP before Vacuum Assisted Resin Transfer Molding (VARTM) the first stage starts with the careful arrangement and stacking of carbon fiber sheets or prepregs in a mold to create the desired composite structure. This process is crucial for achieving the desired fiber orientation and ply alignment, ensuring optimal mechanical properties in the final CFRP composite.

Consolidated Thickness Calculation: Carbon fabric weight = 220 g/m2 Weight converted to consolidated thickness = 0.22 mm per layer(220/1000).

Number of Carbon Fiber Sheets Used = 15 sheets of carbon fiber used

Thickness of one layer: 0.22 mm Total thickness of 15 layers (15 × 0.22) = 3.3 mm

Approximate Total Thickness of Composite Casted Using VARTM =3.7 mm (Approx)

Number of Epoxy Layers = 16 layers of epoxy used

Thickness of Epoxy Layers: - Difference between total composite thickness and carbon fiber sheet thickness: 3.7 - 3.3 = 0.4 mm - Thickness of one epoxy layer: 0.4 mm / 16 layers = 0.025 mm

Cutting and fabrication Process for Carbon Fiber= - 3K, 22 twill weaved carbon fiber fabric cloth cut into 15×15 cm squares - Surfaces of the squares cleaned with acetone - Squares heated in an air oven to 100°C -VARTM process is carried out next.

S.No.	Algorithm
1	CF + Epoxy + Hardener
2	CF + Plastic Added (10/90) PC/ABS Epoxy + Hardener
3	CF + Plastic Added (30/70) PC/ABS Epoxy + Hardener
4	CF + Plastic Added (70/30) PC/ABS Epoxy + Hardener
5	CF + Plastic Added(50/50) PC/ABS Epoxy + Hardener
6	CF + Plastic Added(90/10) PC/ABS Epoxy + Hardener
7	Silanized Graphene Oxide (0.5g/l) CF + Epoxy+ Hardener
8	Silanized Graphene Oxide (1 g/l) CF + Epoxy + Hardener
9	Silanized Graphene Oxide (1.5g/l) CF + Epoxy/ + Hardener

Table 3.1: Sample Composition

3.3 Vacuum-Assisted Resin Transfer Molding (VARTM)

In order to facilitate the resin infusion process, this method calls for the utilisation of a vacuum. VARTM makes it possible to manage the flow of resin and lowers the possibility that the composite will have areas that are either resin-rich or dry. Modifying aspects of the procedure such as the viscosity of the resin, the length of time required for infusion, and the pressure exerted by the vacuum can enable the process to be adapted to fulfil individualised design specifications. Because of its versatility, VARTM has become a popular and successful method for producing CFRP composites of high quality and with constant mechanical properties.

A dry fibre preform or a stack of carbon fibre sheets is positioned on a glass plate in order to carry out the VARTM procedure. To improve the composite part's quality as well as its overall performance, a mesh and fabric material are placed in the part. While in order to give the composite structure the necessary strength and stiffness, a fabric that is commonly formed of carbon fibre or other reinforcing elements is utilised.During the process of infusion, the mesh, on the other hand, performs the function of a flow medium to ensure a uniform distribution. After this, a procedure known as vacuum bagging is performed, in which the bags are sealed snugly while ensuring that there is no air in between the layers, and then they are connected to a source of vacuum. The mould is then subjected to the hoover in order to remove all of the air inside of it, which results in a pressure difference. In addition to removing air from the sealed bag and slowing flow, the vacuum pump generates a vacuum within the bag itself. Once the mould has been placed under vacuum, DGEBA resin is injected into the mould (through the resin infusion connectors, which have also been strategically located for simple resin entrance and exit), and the vacuum assists in drawing the resin through the fibre reinforcement.

The complete impregnation of the carbon fibre reinforcement with resin is the final product of the VARTM process. The vacuum assists in the uniform distribution of the resin throughout the fibre preform, which ensures that the fibre is properly soaked and that any voids are filled. Because of this, the resin is distributed evenly throughout the CFRP composite, which contributes to an increase in the end product's overall strength as well as its stiffness and longevity. Following the soaking of the carbon sheets, resin will flow to the output pipes, where the gate valves will then be closed.

At this point, clamping is performed to secure the intake and output ports and stop any gas leakage that may have occurred. After this step, the vacuum pump is switched off, and the composite is left to cure for a further 24 hours.

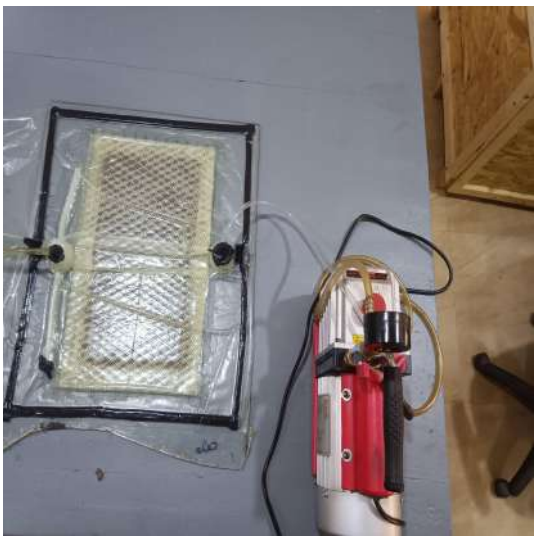

Figure 3.3: VARTM Setup

3.4 CryoTreatment of CFRP Sample:

Cryotreating samples made of CFRP (Carbon Fibre Reinforced Polymer) is a specialised procedure that entails exposing samples to extremely low temperatures. As a result, the samples' mechanical qualities and overall performance are improved. The CFRP samples are prepared for this treatment by first being placed in an environment that is both regulated and isolating, specifically, inside of an aluminium foil bed that is filled with liquid nitrogen '[15].

Before beginning the cryotreatment process, the CFRP samples must first be meticulously prepared. The sample pins are safely encased in a nylon cloth and then tied off with strong knots so that they can be dipped without coming into direct contact with the cryogenic medium.

After the samples have been submerged for a period of twelve hours within. During this time, the cryobath is kept at a temperature of less than -100 degrees Celsius in order to provide the CFRP samples with an exceptionally cold environment.

Monitoring the amount of nitrogen present in the cryobath at all points during the cryotreatment process is an absolute necessity in order to guarantee that the samples are kept at an appropriate depth of submersion. This is often done at regular intervals, such as every four hours, in order to maintain the temperature

that is wanted and maximise the effects of the cryo therapy.

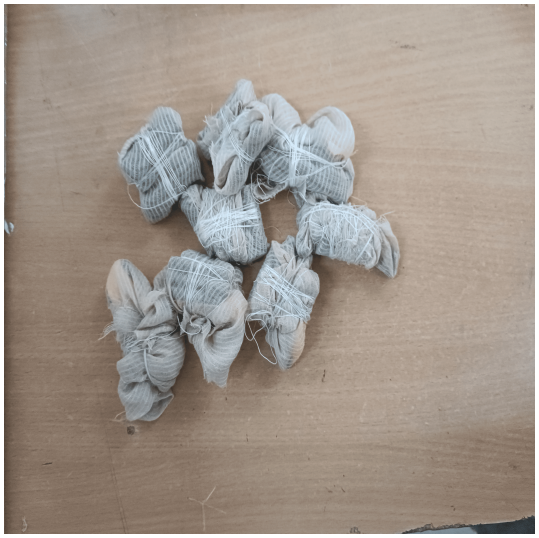

Figure 3.4: Tied Sample

Figure 3.5: Cryo Setup

3.5 Data Collection and Preparation for CFRP Using Pin-on-Disk:

After fabricating and manufacturing of CFRP which are now made in 15 compositions, to study the tribological properties of this sample, Pin on Disk(POD) is performed and an overview of the process is:

3.5.1 Sample Preparation:

The CFRP samples that are currently being manufactured are milled on a CNC milling machine into the shape of thin discs measuring 6 millimetres in diameter. Because of the enormous number of samples that need to be cut and the fact that all of the other possible alternatives, such as laser machining, drilling, and cutting, have already been completed, the most desirable option is CNC machining because of its adaptability, high precision, cost effectiveness, low material loss, and ease of handling.

Emery paper with a grit of between 100 and 600 is used to give the disc samples that have been cut a smoother finish‘[4]. This is done by removing any protrusions of fibres that may have been caused by the cutting process. After that, the samples are attached onto a mild steel rod with a diameter of 6 mm and a height of 35 mm using flexi quick. In order to ensure a smooth and even contact between the samples' flat surface and the POD disc, the flat surface of the CFRP pin is also machined evenly with 600-grit emery paper. This is done in order to ensure smooth and even contact. Flatness is also evaluated for a second time in order to guarantee uniformity across all of the compositions and samples.

3.5.2 Experimental Setup:

In the experimental setup often referred to as the Pin-On-Disk (POD), the prepared sample compositions are fastened in a safe manner to a lever that is kept in place. The lever acts as a platform for the regulated application of normal load and makes it easier for the samples to slide against one another when they are in touch with one another. This enables the examination of a variety of metrics, including friction coefficients and wear rates, among other things.

In order to conduct out the experiment, a pin-on-disk apparatus is utilised. This equipment consists of a rotating disc that moves down a track while a sample pin that is linked to it remains stationary. Because the rotating disc is attached to a rotating shaft or spindle, it is able to rotate in a regulated manner and slide down the shaft. On the other hand, the pin will not move from its current position and will continue to serve as a contact point for the mobile disc.

Because of this configuration's ability to accurately imitate the frictional interaction that occurs between two surfaces, it is much simpler to measure the frictional forces and wear rates. The lever allows for precise manipulation of the variables in the experiment, which helps to maintain consistency and ensure the repeatability of the findings. In addition, important variables, including the usual load, sliding speed, and sliding distance, are determined in accordance with the experimental design so that an exact calculation of the desired results may be made.

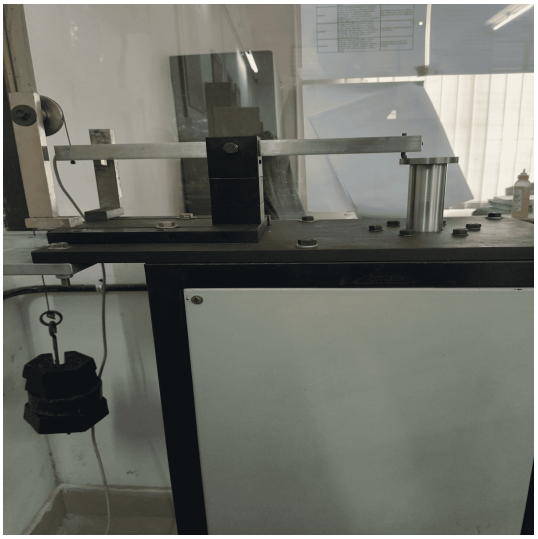

Figure 3.6: Tribological Setup-P.O.D

3.5.3 Data collection in Pin on Disk(POD):

During the POD experiment for CFRP, the friction force was continuously measured and recorded at a frequency of one measurement per second as part of the data-gathering process. This was done for each individual circumstance involving RPM (rotations per minute) and Load. As a result of this, precise and time-resolved data on the frictional behaviour of the pin and the disc are being gathered as a result of this. Because of this, it follows that the researchers would be able to analyse the dynamic changes in friction if they were to record the friction force over time. Additionally, they would be able to explore the link between RPM, COF, wear, and the observed frictional forces.

In a nutshell, a comprehensive investigation of the sample is being carried out for its tribological properties during this step of the data collection and preparation stage of the Pin on disc approach for CFRP. This stage involves the meticulously

controlled experiment and precise data collecting. As a result, acquiring data that provides insights into the friction wear and features of the CFRP materials.

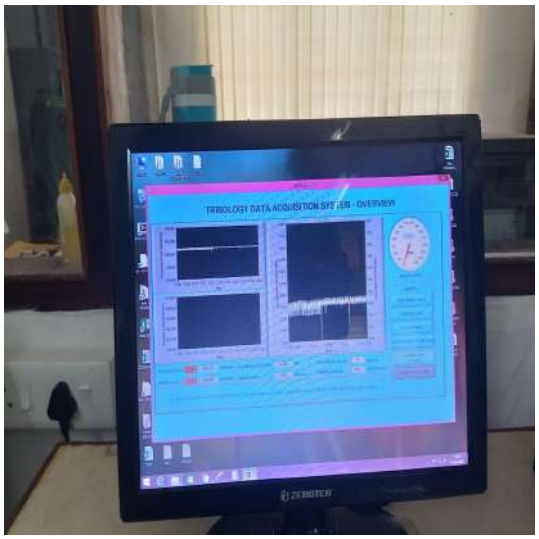

Figure 3.7: POD Data Collection

3.5.4 Data Analysis and Interpretation:

To gain meaningful insights on data and its analysis and interpretation, a thorough analysis of how data behaves and acts is being done. For such an insights to be developed several statistical analysis techniques are carried out to uncover any trends patterns and influence of meaningful parameters for example like coefficient of friction and wear rate. Through such techniques, the hidden relationship between various variables and statistical significance of various patterns are thus obtained thus signifying the performance of CFRP composites.

After understanding the relationship between them, comparison are being done which can be made between different samples, parameters, or experimental conditions to evaluate the performance of CFRP composites.By analyzing and comparing the collected data, we can now assess the effectiveness of different compositions, load levels, RPM settings, or other factors on the coefficients of friction and wear rate. Through this stage, the result of data analysis and interpretation provide key information which can even be used for prediction behavior of CFRP composites that can be used in real world scenarios. This thereby leads to understanding key relationship, which researchers can use to make informed decisions regarding the design, optimization, and selection of CFRP composites that can thus be used for aerospace and other applications.

3.6 Machine Learning and Neural Network Based Development:

Developing machine learning and neural network models that can accurately predict the behaviour of CFRP (Carbon Fibre Reinforced Plastic) composites is the issue at hand. The goal is to construct a highly accurate model to predict the wear characteristics and coefficients of friction of CFRP by training and validating the experimental data under various experimental conditions, including sample composition, load, and RPM.

Consequently, the objective is to utilise the potential of artificial intelligence, machine learning, and artificial neural networks to develop a predictive model that can provide insight into the performance characteristics of CFRP composites.By training the neural network with the collected data, we hope to develop a model that can generalise well and accurately predict friction coefficients and wear rates under novel experimental conditions. This capability will be useful for optimising the design and performance of CFRP composites used in aerospace applications.

For successful deployment various stages include:

1:Data Preparation: Preprocess the collected data from the pin-on-disk experiment, including Load, Sliding Distance, RPM friction force and wear measurements. This may involve selecting an appropriate and accurate area in the time series column to which other parameters remain constant, for this data during the time of 6 Minute to 7 Minute chosen(During this time data remained constant). The next step involves data cleaning, normalization, and splitting into training and testing sets.

2. Feature Selection:In this phase, the focus is on determining the input variables or features that have the most significant impact on the coefficients of friction and wear rate of CFRP composites. The analysis considers factors such as sample compositions, load, RPM, and Time series and by applying statistical analysis techniques and exploring the collected data, this thereby helps us to understand key variables that strongly influence the coefficients of friction and wear rate. The process involves examining correlations, conducting hypothesis testing, and evaluating the statistical significance of different factors.

The important features are selected based on their contribution to the variations

in the coefficients of friction and wear rate. These features serve as inputs to the neural network model and play a crucial role in accurately predicting the behavior of CFRP composites.

By identifying the relevant features, we can now gain valuable insights into the underlying mechanisms that affect friction and wear characteristics.

3. Architecture Design: During this stage, an appropriate machine learning model is to be chosen based on the complexity of the problem and data behavior. For a neural network model, several factors are considered such as the number of hidden layers, number of neurons per layer, the selection of activation functions, and in training and incorporation of regularization techniques. In a machine learning model, the factors include hyperparameter tuning, scalability, performance metrics, to name a few.

For successful deployment various stages include

- Data Preparation:

  Process the collected data from the pin-on-disk experiment, which includes measurements of Load, Sliding Distance, RPM friction force, and wear. This may entail selecting an appropriate and precise area in the time series column where other parameters remain constant, for this data during the time period selected (6 Minutes to 7 Minutes; data remained constant during this time period). Next, data is cleaned, normalized, and divided into training and testing sets.

- Feature Selection:

  In this phase, the priority is put on identifying the input variables or characteristics that have the greatest influence on the coefficients of friction and wear rate of CFRP composites. By employing statistical analysis techniques and examining the collected data, the analysis takes into account variables such as sample composition, load, RPM, and time series. This enables us to comprehend the variables that have the greatest impact on the coefficients of friction and wear rate. Examining correlations, verifying hypotheses, and assessing the statistical significance of various factors comprise the process. The important features are selected based on their contribution to the variations

in the coefficients of friction and wear rate. These features serve as inputs to the neural network model and play a crucial role in accurately predicting the behavior of CFRP composites.

By identifying the relevant features, we can now gain valuable insights into the underlying mechanisms that affect friction and wear characteristics.

- Architecture Design:

  During this phase, a suitable machine learning model is selected based on the problem's complexity and the behavioral characteristics of the data. Several factors, such as the number of hidden layers, the number of neurons per layer, the choice of activation functions, and the training and incorporation of regularisation techniques, are considered for a neural network model. Among the factors in a machine learning model are hyperparameter optimization, scalability, and performance metrics.

3.6.1 Machine Learning based architectures:

To deploy and enhance the performance of any model, the following measures must be taken: Selecting the optimal values for the parameters that characterise the behaviour of the machine learning model constitutes hyperparameter tuning. These parameters can have a substantial effect on the efficacy and generalizability of the model. Several techniques include grid search, random search, and node adjustment.

Scalability is an additional crucial step, particularly if the dataset is large or is anticipated to expand over time. This phase is essential for enhancing performance while dealing with large amounts of data. Metrics of performance play a crucial role in evaluating the performance of a model and determining its applicability to the problem at hand. Metrics such as accuracy, precision, recall, F1 score, and mean squared error (MSE) are frequently employed to evaluate the predictive capabilities of a model. The selection of performance metrics depends on the problem's specific objectives and requirements. Additionally, during the architecture design phase, factors such as interpretability, computational resources, and the availability of labeled data are considered.

The objective of the architecture design phase is to choose a machine learning model capable of handling the problem's complexity, utilizing the available data,

and delivering accurate predictions or valuable insights. By taking into account factors such as hyperparameter tuning, scalability, and performance metrics, we can select a model that best meets the criteria for accurately predicting the target.

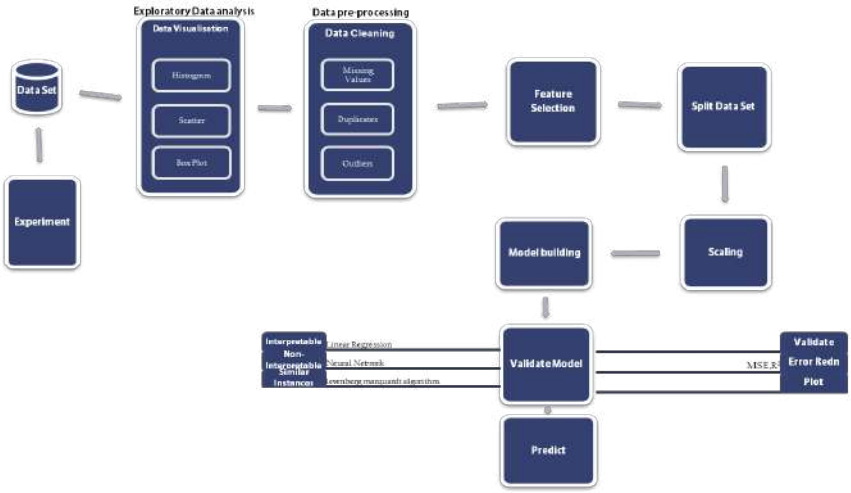

Figure 3.8: Machine Learning

3.6.2 Neural Network prediction

The complexity of the relationship between the input variables and the coefficients of friction and attrition rate has a significant impact on the number of hidden layers and neurons per layer in neural network models. Complex problems may necessitate architectures with a greater number of neurons to capture intricate data patterns and nonlinearities. In this scenario, however, since a shallower architecture is being considered, optimal data fitting may suffice.

The choice of activation functions is crucial for determining how network neurons transform input signals into output values. Common activation functions include sigmoid, ReLU, and tanh, each of which has its own properties and applicability to various data types and problem domains.A combination of three layers has been proposed to address the complexities of this issue.

Regularisation techniques, such as dropout or L1/L2 regularisation, may be utilised to prevent overfitting and enhance the neural network model's generalisation

capability. These techniques reduce the influence of irrelevant or chaotic features and improve the model's performance on unseen data.

The objective of the phase of architecture design is to establish a balance between model complexity and generalization performance. It requires thoughtful consideration of the issue at hand, the available data, and the desired level of model precision. By selecting a suitable neural network architecture, we can optimize the model's ability to capture the relationships between the input variables and the coefficients of friction and wear rate, resulting in accurate predictions and insightful insights.

Using the prepared data and the trained data, these models are then constructed. This supervised learning module uses several techniques, including backpropagation, hyper parameter, and gradient descent, to optimise the model based on its types. The model's efficacy can then be enhanced by adjusting the learning rate and batch size.

Now, evaluate the efficacy of the trained neural network model using evaluation metrics such as mean squared error, precision, or other pertinent metrics. Compare the model's predictions with the pin-on-disk experiment's actual coefficients of friction and wear rate.

Document the machine learning modules and neural network architecture in the final phase, including the number of layers, neurons, activation functions, tunings, and any other information pertinent to the design and implementation of the model.

Chapter 4

MATERIALS USED AND TEST SETUP:

4.1 Materials Used

This study uses the thermoset polymer matrix epoxy YD 128, Aditya Birla Chemicals Ltd., Thailand, with an EEW of 185 to 194 g/eq. Modified TH 7301 (Aditya Birla Chemicals Limited, Thailand), a cyclo aliphatic amine, cures. DGEBA matrix modification (ABS, Cycolac MG 47F, Sabic, Saudi Arabia) is done by melting polycarbonate (PC, Makrolon 2856, Covestro AG, Germany) and poly (acrylonitrile butadiene styrene). 3K authentic carbon fibre fabric cloth, 220g/m2, 2x2 Twill Weave, Manufacturer Part No. CBC24030, Carbon black Composites, India, reinforces the composite material.

4.1.1 Carbon Fabric Cloth:

For the experimental study, 2x2 Twill weave Carbon Fiber Fabric is used. The material carries a 220g/m2 while exhibiting an Izod impact strength of 612J/m.

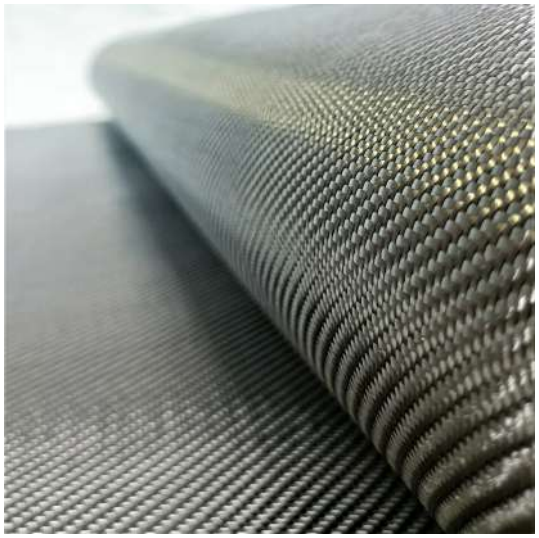

Figure 4.1: Carbon Fiber Cloth,courtesy:(Indiamart.com)

4.1.2 Epoxy Resin:

1. Appearance:

   The epoxy looks as a clear, colorless to light yellow liquid when visually inspected.

2. Epoxy Equivalent Weight:

   The epoxy equivalent weight, measured according to ASTM D 1652-04, falls within the range of 185 to 194 grams per equivalent. This parameter provides information about the average molecular weight of the epoxy resin.

3. Epoxide Value:

   The epoxide value, determined by ASTM D 1652-04, ranges from 5.15 to 5.40. This value indicates the number of epoxy groups present in the resin per 100 grams of resin. It reflects the epoxy resin's reactivity and crosslinking potential.

4. Hydrolyzable Chlorine:

   As per ASTM D 1726-03, the hydrolyzable chlorine content is 0.05% or below. This parameter assesses the presence of chlorinated compounds that may impact the epoxy's chemical stability.

5. Flash Point:

The flash point, determined using ASTM D 93, is measured at 252℃. This value represents the minimum temperature at which the epoxy vapors can ignite when exposed to an open flame or spark.

6. Viscosity at 25℃:

   The viscosity of the epoxy at 25℃, determined by ASTM D 2196-05, falls between the range of 11,000 to 14,000 centipoises (cPs). Viscosity indicates the epoxy's resistance to flow and can influence its processing and application.

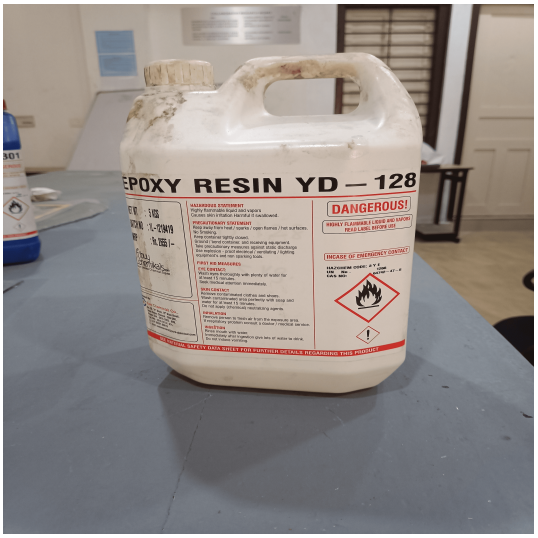

Figure 4.2: Epoxy resin

4.1.3 Hardener:

A TH 7301 Hardener is used for sample preparation.

1. Odor:

   The hardener has an amine odor, characteristic of amine-based curing agents.

2. Amine Value:

   The amine value of the hardener, determined by DIN 16945, ranges from 260 to 285 milligrams of potassium hydroxide (KOH) per gram. This value indicates the amount of amine groups present in the hardener and provides information about its curing potential.

3. Flash Point:

The flash point of the hardener, measured using ASTM D 93, is 100℃. This value represents the minimum temperature at which the hardener vapors can ignite when exposed to an open flame or spark.

4. Glass Transition Temperature:

   The glass transition temperature of the hardener, determined by DIN 11357, is 50℃. This temperature signifies the point at which the hardener transitions from a glassy to a rubbery state, indicating its ability to contribute to the overall strength and toughness of the cured epoxy.

5. Density at 25℃:

   The hardener's density, measured according to ASTM D 1475-98, is reported as 1.03 grams per cubic centimeter (g/cc) at 25℃. This parameter provides information about the hardener's mass per unit volume.

6. Pot Life at 25℃:

   The pot life of the hardener, determined by TEC-AS-P-111, ranges from 28 to 45 minutes at 25℃. This indicates the maximum time available for mixing and applying the epoxy resin before it begins to cure and solidify.

Figure 4.3: Hardener

4.1.4 Thermo-Plastic Modifiers Polycarbonate (PC):

The properties of these Makrolon 2856 virgin quality polycarbonate can be summarized as in the Table ‘4.1:

Table 4.1: Properties of Thermo-Plastic Modifiers Polycarbonate (PC)

Sl.No	Property	Standard
1	Specific gravity	1.20 g/cm3 (ASTM D 792)
2	Coefficient of thermal expansion	0.65 × 10-4/℃ (ISO 11359-1, -2)
3	Notched Izod impact strength	70 kJ/m2 (ISO 7391/b.o. ISO 180-A)
4	Glass transition temperature	145℃ (ISO 11357-1, -2)
5	Tensile stress at yield	65 MPa (ISO 527-1, -2)
6	Tensile strain at break	130% (ISO 527-1, -2)
7	Flexural stress	97 MPa (ISO 178)
8	Melt temperature	280 - 320℃

Figure 4.4: Poly Carbonate

4.1.5 Acrylonitrile Butadiene Styrene (ABS):

The Table ‘4.3 ,ABS, a commonly used thermoplastic polymer, exhibits mechanical properties such as good impact resistance, and thermal stability. Thus they can be used as reinforcement material in CFRP along with PC. The improved properties also show properties like improved toughness, impact resistance, and dimensional stability. ABS fibers can be aligned in the desired direction to provide reinforcement along specific load-bearing areas, enhancing the strength and stiffness of the composite structure.

Table 4.2: Acrylonitrile Butadiene Styrene (ABS)

Sl.No	Property	Standard
1	Specific gravity	1.20 g/cm3 (ASTM D 792)
2	Coefficient of thermal expansion	8.82E-05 /℃ (ASTM E 831)
3	Notched Izod impact strength	320 J/m (ASTM D 256)
4	Vicat softening temperature	98℃ (ISO 306)
5	Melt temperature:	220 - 260℃

Table 4.3: Acrylonitrile Butadiene Styrene (ABS)

4.1.6 Infusion Mesh:

The infusion mesh is a consumable component used to facilitate the resin infusion procedure during the production of CFRP (Carbon Fibre Reinforced Polymer) composites.The infusion mesh is utilised during the infusion procedure based on the Table 4.5, specifically in Vacuum-Assisted Resin Transfer Moulding (VARTM). Its purpose is to improve resin flow and fabric impregnation by facilitating resin gliding within the hoover bag. This is especially advantageous for larger moulds and resin infusions with medium viscosity.

The infusion mesh plays a vital function in ensuring the uniform distribution of resin throughout the carbon fibre fabric. It ensures that the resin flows smoothly and uniformly across the complete mould by distributing it evenly. By providing channels for resin flow, the infusion mesh prevents the formation of dry patches or voids in the composite, which could compromise its structural integrity.

Table 4.4: Infusion Mesh

Sl.No	Parameter	Specfications
1	Color	White
2	Material	HDPE
3	Width	White

Table 4.5: Infusion Mesh

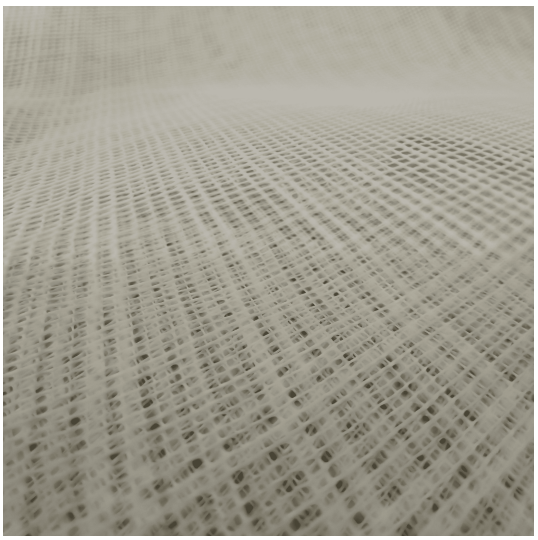

Figure 4.5: Infusion Mesh

4.1.7 Peel Ply fabric:

In order to absorb excess resin during the composite layup procedure, peel ply fabric is utilised. By absorbing excess resin, this procedure ensures that the carbon fibre layers are properly wetted and reduces the likelihood of resin pooling or excessive resin content. In addition, they prevent and function as barriers between the composite surface and other substances or contaminants. In addition, they aid in preventing contamination from a variety of tools, release agents, and other extraneous substances that can compromise the bonding and surface quality of CRP laminates.

The polyester Nylon 6 peel-ply fabric utilised here has a width x thickness of 1000nm x 85GSM.

4.1.8 Vacuum Bagging Film:

By using a vacuum-sealed film, applying uniform pressure, and consolidating the composite material during the curing process, the process achieves the desired results. The vacuum Bagging is then sealed, and by removing air with a vacuum source, a vacuum environment is created around the composite.

Figure 4.6: Peel Fabric

Figure 4.7: Vaccum Bagging Film

4.1.9 Sealant Tape:

Sealant Tape is used to produce a reliable and airtight seal between the vacuum bag and the mould surface. The tape therefore prevents any air leakage or vacuum loss during any vacuum bagging process and ensures a tight seal is created between the vacuum bag and mould, thereby eradicating the possibility of air ingress and the formation of voids in the composites.

Butyl-sealant Tape is the sealant tape used here.

Figure 4.8: Sealant Tape

4.1.10 Infusion Resin Connector:

During the infusion process, serving as a pathway or channels for the resin to enter and depart the mould. To facilitate the passage of resin throughout the layup process, connectors must be precisely positioned in a particular location on the mould during placement. The connector utilised in the experiment is a PVC-based connector with a diameter of 8mm.

Figure 4.9: Connector

4.1.11 Hose Pipe:

A hose pipe is used to facilitate the smooth flow of resin into and out of the vacuum bag and to effectively create a vacuum within the vacuum bag. In this instance, an 8mm-diameter vacuum pump is utilised so that resin and air can be drawn in and out of the vacuum created with greater efficiency.

Figure 4.10: Hose Pipe,courtesy:(Meesho)

4.1.12 Vacuum Pump:

By establishing a negative pressure environment within the Hoover bag or mold. The procedure eliminates air and gases from the mold, resulting in a constant pressure differential and a continuous flow of resin into the carbon fiber reinforcement. The vacuum pump used in the experiment has a displacement of 113L/Min and a capacity of 2.5 CFM.

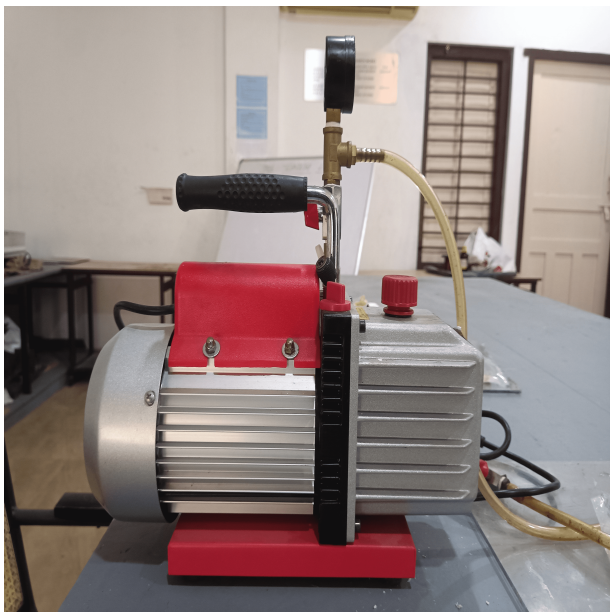

Figure 4.11: Vaccum Pump

4.1.13 Aluminum Foil Insulated Bath:

A container insulated with aluminium foil is utilised for cryo-bathing CFRP (Carbon Fibre Reinforced Polymer) materials. During the cryogenic treatment procedure, they serve as a thermal barrier to preserve a low-temperature environment. This bag is constructed with layers of aluminium foil insulation that minimise heat transfer and maintain a constant low temperature for CFRP samples during cryo immersion. This insulation ensures that the cryo-bathing procedure is carried out effectively, thereby contributing to the improvement of the mechanical properties and performance of CFRP materials.

Figure 4.12: Aluminum Foil Insulated Bath

4.2 Experimentation

4.2.1 Pin on Disk Experiment

Pin on disc is an instrument of tribological testing apparatus used to assess the wear resistance of materials. By utilizing the device, the wear resistance and friction coefficient of Carbon Fibre Reinforced Polymer (CFRP) composites can be determined. By examining the material's tribological properties, we can determine its durability and dependability in various situations. In addition to aiding in the optimization of which composition is optimal.

To evaluate the tribological properties of CFRP composites in accordance with ASTM G 99, a Pin on Disc (POD) experiment is conducted. The sample, which has the shape of a Disc with a diameter of 8 mm, is first affixed to a mild steel cylinder with a height and diameter of 3.5 cm by 8 mm. The contacting surface was a disc of hardened alloy steel with a surface roughness (Ra) of 0.43 m and a hardness of 70 HRC..This is because pin wear rate is small'[28] as the pin polished before loading.

In separate experiments, loads of 20 kN, 40 kN, 60 kN, and 80 kN were applied. The next stage is to vary the parameters, Rotation Per Minute (RPM), which are varied between 1 m/s, 1.5 m/s, and 2 m/s, with a fixed duration of 10 minutes for each experiment. Sample output parameters, namely the coefficient of friction and wear rate, were determined through experimentation.
In conclusion, a comprehensive investigation of the friction and wear properties of CFRP composites under varying loads and sliding conditions was conducted using POD. The results of the experiment will provide additional information regarding the use of CFRP composites in applications where wear resistance and failure prevention are crucial.

4.2.2 Sputter Coater Device:

The Sputter Coater is utilized to apply an ultra-thin coating onto the surface of CFRP (Carbon Fiber Reinforced Polymer). Gold (Au) is the chosen coating material. With gold as the coating material, it enhances the image quality by improving

the reflectivity of the material sample. In short, the process helps in sharpening the visibility of damages on the sample, enabling better observation and analysis.

Figure 4.13: Gold Sputter Coating Device

4.2.3 Metallurgical Microscope:

The metallurgical microscope is used to evaluate samples of CFRP that have been coated with gold. This microscope has been fitted with specialised features and imaging techniques that allow for an in-depth analysis of the microstructure, composition, and surface properties of the sample. By employing brightfield, darkfield, and polarised light techniques, the microscope enhances the contrast and clarity of the metal's various features, thereby facilitating the examination of the sample's characteristics. Consequently, a metallurgical microscope is a valuable instrument for evaluating the quality, integrity, and performance of CFRP materials '[21].

Figure 4.14: Metallurgical Microscope

Chapter 5

RESULT AND DISCUSSIONS

5.1 Experimentation and Analysis

On the basis of FTIR and SEM analysis, the formation of a flexible Si-O-Si bond and the distribution of SGO particles were revealed; [18]. Similarly, for the PC/ABS modified CFRP composites, FTIR, DSC, and SEM analyses have confirmed the chemical modification and reaction of thermoplastic (TP) modifiers on DGEBA resin.

5.1.1 RT Impact on the effect of force on wear and coefficient of friction:

Through the Pin on Disk experiment, tribological study was conducted. The test condition was such that samples were placed under varying loads of 20N, 40N, 60N and 80N while keeping a sliding speed constant of 1 m/sec.

5.1.1.1 Impact on the effect of force on coefficient of friction:

As shown in the Fig ‘5.1 as the concentration of S.G.O increased from 0.5 to 1.0, relative to the Neat sample, the coefficient of friction tends to decrease and reaches a minimum of 0.17.Due to the inherent lubricating properties of graphene oxide, the coefficient of friction can be reduced by a maximum of 25 percent. Further increase in S.G.O concentration indicates that C.O.F has resumed its ascent. This indicates the optimal concentration (in this case, 1.0) at which the maximum C.O.F. reduction is attained. Beyond this concentration, the lubricating effect of S.G.O may diminish, leading to an increase in the coefficient of friction.

In CFRP (Carbon Fibre Reinforced Polymer), PC (Polycarbonate) demonstrates

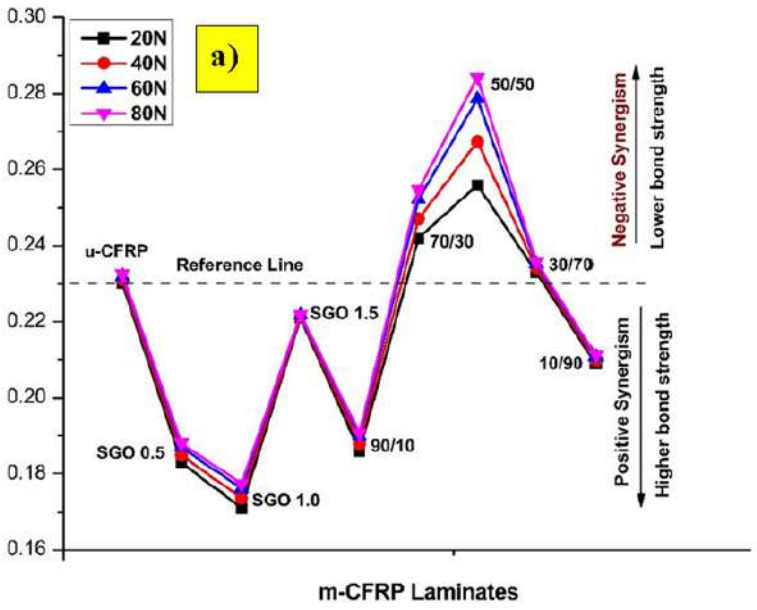

Figure 5.1: Effect of Force on Coefficient of Friction

greater stiffness and strength than ABS (Acrylonitrile Butadiene Styrene). When PC and ABS are combined in a composition, a synergistic effect occurs '[16], resulting in enhanced mechanical and thermal properties. The reason they exhibit such a property is because the combination capitalises on the strength of the PC and the flowability of the ABS.This positive synergism effect is more pronounced in blends with a ratio of 90% PC to 10% ABS (90/10), while it is least pronounced in blends with a ratio of 50% PC to 50% ABS (50/50).In a nutshell, PC/ABS 90/10 demonstrated the greatest C.O.F. reduction, whereas 50/50 demonstrated the least.

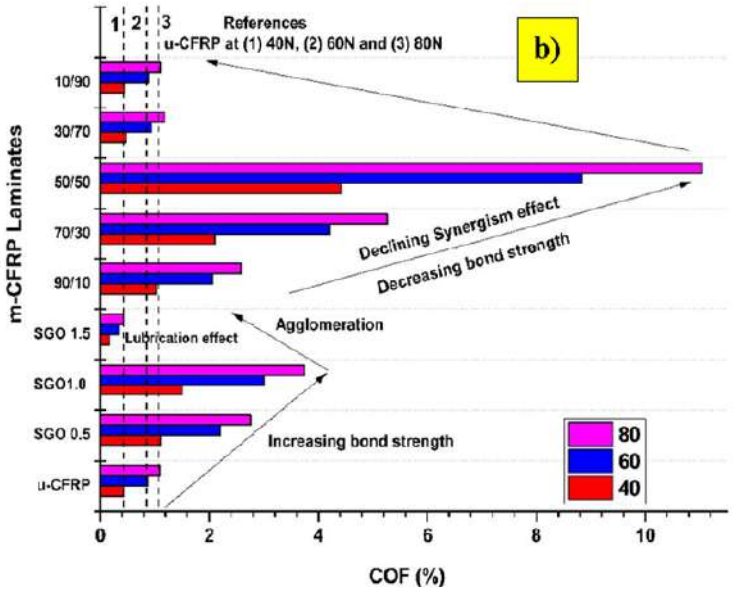

Figure 5.2: % Effect of Force on Coefficient of Friction

From the fig ‘5.2 As the load increases, so does the contact area between the disc and the sample. This results in increased pressure and shear forces at the contact interface, which, in the case of S.G.O., can degrade any lubricating film that may have formed at the contact surface. As depicted in Fig. c, this increase in contact area results in a higher coefficient of friction (COF) and can even cause an increase in the wear rate (WR) of the materials.

From the fig ‘5.2, Due to the diminishing synergism effect “[16] and decreased bond strength between PC, ABS, and PC/ABS when using DEGBA epoxy, there is less interaction between the bonds in the case of PC/ABS blends. This translates to a greater percentage increase in the coefficient of friction for the 50/50 mix as the load increases. In contrast, the other mixtures exhibit superior agglomeration phenomena and enhanced bond strength, resulting in smaller COF increases.

The burden increase did have an effect on the tribological properties of the materials. The contact area, lubrication, and bond strength play significant roles in determining the coefficient of friction variations. To optimise the tribological performance of materials, it is necessary to consider these factors when analysing their behaviour under variable stresses.

5.1.1.2 Effect of Load on Wear characteristics:

As the COF has a direct effect on the wear characteristics, it is possible to observe analogous tendencies. As depicted in Figure ‘5.3, as the S.G.O composition increases from 0.5 to 1.0, the wear characteristics are diminished. This decrease is attributable to the inherent lubricating properties of the SI-O-SI bonds, which enhance stress absorption and improve the sample’s toughness. However, as the composition increases, the coefficient of friction increases, predominantly due to the occurrence of agglomeration phenomena.”

In PC/ABS compositions, the 50/50 ratio has the maximum wear rate, while the 90/10 ratio has the lowest. This distinction is attributable to the synergistic effect and enhanced bond strength of the PC/ABS composite. The higher compactions and energy redistribution among molecules in the 90/10 composite result in enhanced ductility, which reduces the rate of wear. The 50/50 blend, on the other hand,

exhibits lower molecular interaction, resulting in a more brittle behaviour and, thus, increased wear.

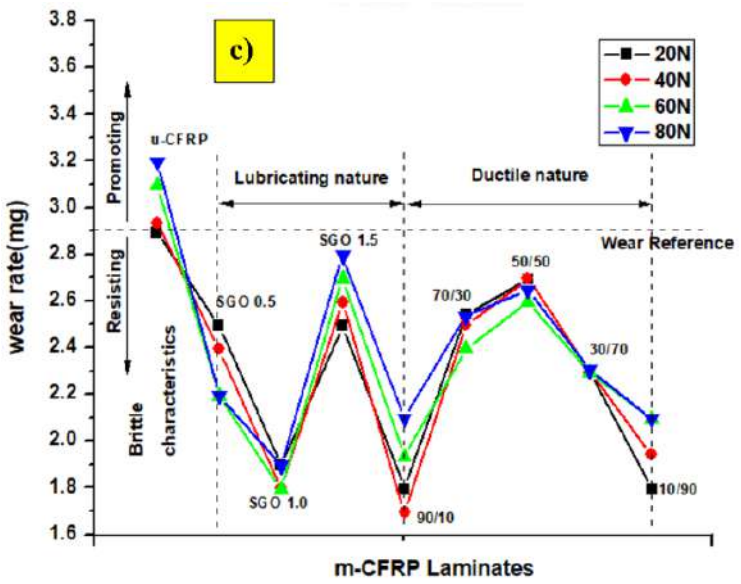

Figure 5.3: Effect of wear characteristics on Coefficient of Friction

‘

5.1.2 Impact on the Effect of wear and coefficient of friction: Based on Sliding velocity

Pin on Disc (P.O.D) experiments were conducted on samples rotating at 298 rpm, 448 rpm, and 558 rpm, which correspond to sliding velocities of 1, 1.5, and 2 (unit in m/s) while the force was held constant at 20 kN and this was done in order to determine the influence of sliding velocity on attrition and coefficient of friction.

5.1.2.1 Effect of Sliding velocity on Coefficient of friction:

As the speed of each sample increased,from the fig ‘5.4 COF decreased and WR increased, following the same pattern as the effect of force. Sample SGO 1.0 exhibited the lowest COF, measuring 0.17, while sample 50/50 exhibited the highest COF, measuring 0.29. As the PC concentration increased, however, a minimum COF of 0.21 was detected in sample 10/90. In addition, samples 70/30, 50/50, and 30/70 demonstrated an increase in COF relative to uCFRP, whereas samples SGO0.5, SGO1.0, and SGO1.5 demonstrated a decrease in COF relative to uCFRP.

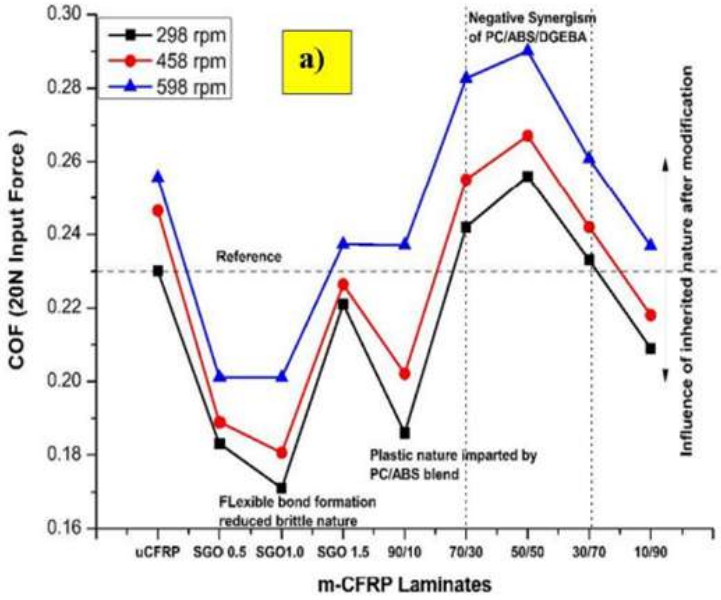

Figure 5.4: Effect of Sliding Velocity characteristics on Coefficient of Friction

During mechanical testing, the strain of the sample controlled the effect of velocity, as sample SGO1.0 and 90/10 with minimal COF also produced maximum strain. From Fig '5.4, it can be observed that C.O.F decreased as speed increased; this was due to the fact that as speed increased, heat generation also increased, resulting in thermal softening of the composite surface, which decreased COF as rpm increased.

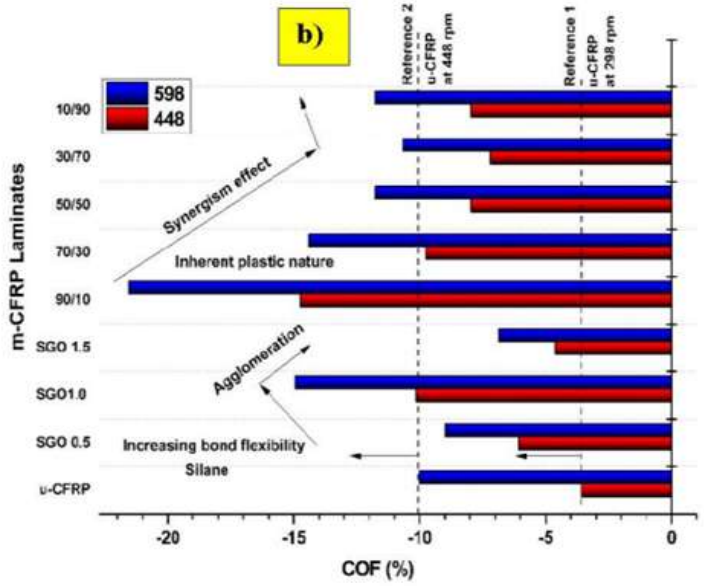

Figure 5.5: % Effect of Sliding Velocity characteristics on Coefficient of Friction

In the case of PC/ABS, the decrease in COF as sliding speed increases is a result of ductile shearing and shredding. The ductile shearing and shredding of plastic zones leads to the formation of more resistant zones in the morphology, thereby

contributing to a lower C.O.F at higher loads ‘5.5.

5.1.2.2 Effect of sliding velocity on Wear:

As shown in fig ‘5.6 , the presence of graphene-coated particulates on the surface of S.G.O (Graphene Oxide)-based CFRP plays a crucial role in reducing wear. Particles of graphene form a lubricating layer between the contact interfaces, thereby reducing friction and wear.The lubricating properties of graphene contribute to the formation of an oil film that functions as an interlayer, thereby enhancing the composition’s wear resistance. This interlayer smoothes the contact surfaces, reducing surface roughness and the likelihood of asperities causing erosion through direct contact. In addition, this formation absorbs and dissipates the energy generated during sliding, thereby preventing excessive heat accumulation and reducing wear.

Therefore, the CFRP composition containing S.G.O at a concentration of 1.0 demonstrates the lowest attrition rate. Nevertheless, when the S.G.O concentration exceeds this threshold, the oil films produced between the contact interfaces tend to break, resulting in an increase in wear rate.

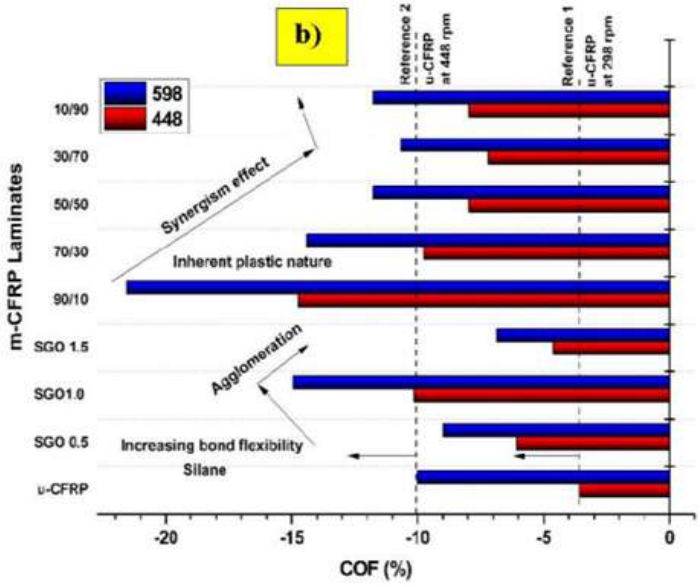

Figure 5.6: Effect of Sliding Velocity characteristics on Wear

In the case of PC/ABS compositions in the fig ‘5.6, the material’s improved ductile shearing and shredding properties play a significant role in reducing wear. At high sliding velocities, the ABS component of the PC/ABS blend elongates and deforms in the rotational direction of the disc, absorbing abrasive shocks and reducing wear. Due to the synergistic effect of the PC and ABS, the PC/ABS

composition with a ratio of 90/10 exhibits a low attrition rate, resulting in enhanced ductility and deformation resistance.

Alternatively, the PC/ABS composition with a 50/50 ratio exhibits a greater wear rate. This is due to the increased presence of debonding between the PC and ABS components, which results in a more brittle structure. The 50/50 composition's lack of ductility and deformation resistance promotes wear and increases the wear rate. As shown in Fig '5.7, the diagrammatic representation of the degradation mechanism of both SGO CFRP and PC/ABS CFRP is briefly described.

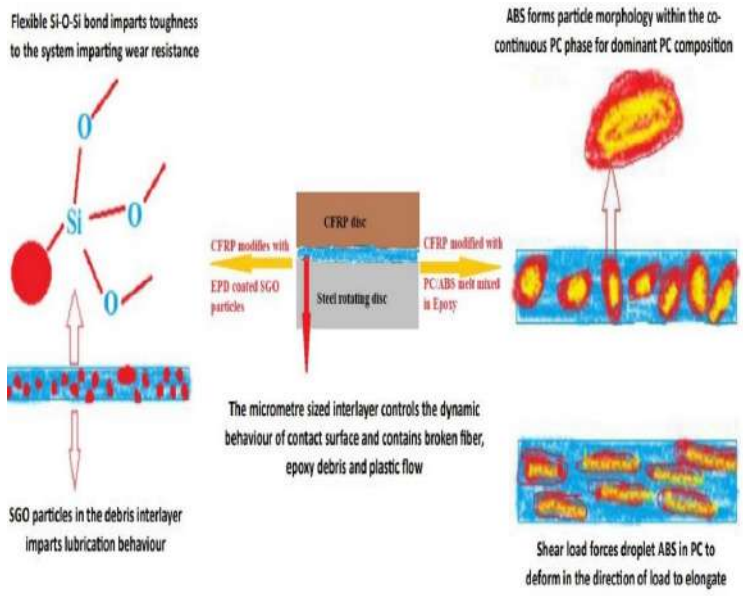

Figure 5.7: Diagrammatical Representation SGO and PC/ABS

5.1.3 CT Impact on the effect of force on wear and coefficient of friction:

5.1.3.1 Impact on the effect of force on coefficient of friction:

As shown in the Fig '5.8 , The coefficient of friction has a tendency to decline and achieves a minimum of 0.17, following the trend as similarly as possible to that of Room Temperature. This is in comparison to the Neat sample, for which the concentration of S.G.O grew from 0.5 to 1.0.This is because the S.G.O forms a thin layer in between, which increases the bonding strength between the two components. However, as the load grows, the bonding in between the components breaks, resulting in a greater surface area coming into contact with the components and the disc, which causes the friction coefficient to rise.

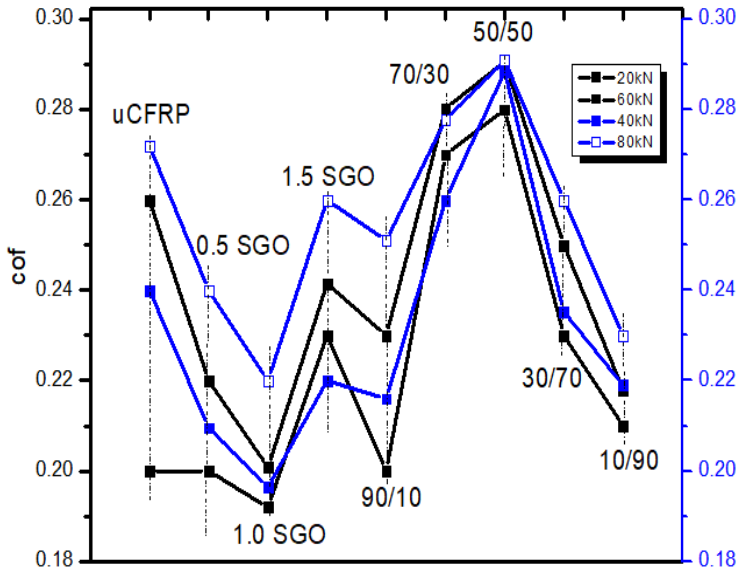

Figure 5.8: CT Effect of Force on Coefficient of Friction

Based on the Fig‘5.8,PC is stiffer and stronger than ABS in CFRP. PC and ABS compositions have synergistic mechanical and thermal qualities. The combination uses the PC's strength and the ABS's flowability.This beneficial synergism impact is strongest in blends with a ratio of 90% PC to 10% ABS (90/10), and weakest in 50/50 mixes.In summary, PC/ABS 90/10 had the most C.O.F. reduction, whereas 50/50 had the least, as seen in Room Temperature. However, when load increases, brittleness increases, which raises coefficient of friction.

5.1.3.2 Effect of Load on Wear characteristics:

For CT conditions the COF directly affects wear properties, hence identical tendencies can be observed. As seen in fig 5.9, S.G.O composition increases from 0.5 to 1.0 reduces wear characteristics. The Si-O-Si bonds' intrinsic lubrication improves stress absorption and sample toughness, causing this drop. Agglomeration events enhance the coefficient of friction as composition increases. Due to bond strength degradation, for higher loads the bond breaks and due to increase in temperature this causes the Si-O-Si bonds to breaks leads to increase in wear.

As seen in the fig 5.9,In PC/ABS compositions, the 50/50 ratio has the highest wear rate under CT circumstances, while the 90/10 ratio has the lowest. PC/ABS composite synergy and bond strength explain this difference. The 90/10 composite's increased compactions and energy transfer among molecules increase ductility, re-

ducing wear. Cryotreatment increases brittleness, therefore the sample wears faster at higher loads.

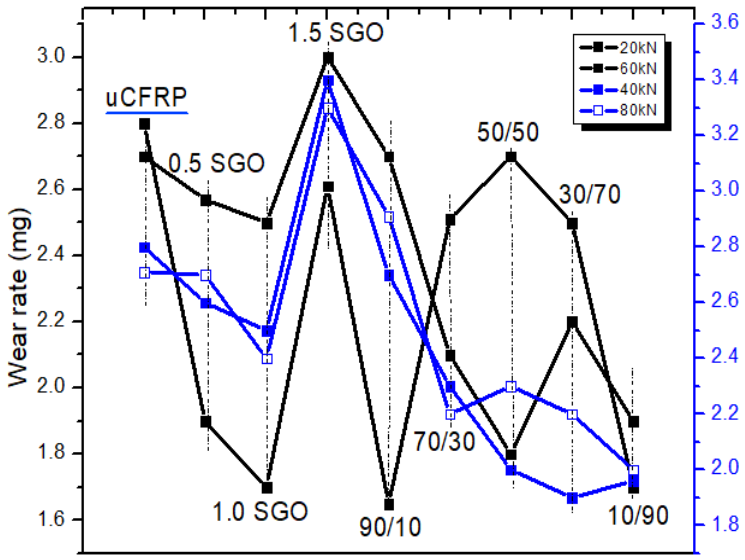

Figure 5.9: Effect of wear characteristics on Coefficient of Friction

5.1.4 Impact on the Effect of wear and coefficient of friction: Based on Sliding velocity

5.1.4.1 CT Effect of Sliding velocity on Coefficient of friction:

In the fig 5.10 CT sample, Since Like force, COF decreased, but the increase of COF can be observed as sample speed increases. For the Sample SGO 1.0 had the lowest COF, 0.17, however as further concentration increases, binding strength decreases and COF increases.

Sample 50/50 had the greatest COF, 0.28. Sample 10/90 had a COF of 0.21 as PC content rose the decrease in cof can be seen. Samples 70/30, 50/50, and 30/70 had higher COF than uCFRP, while SGO0.5, SGO1.0,had lower COF.

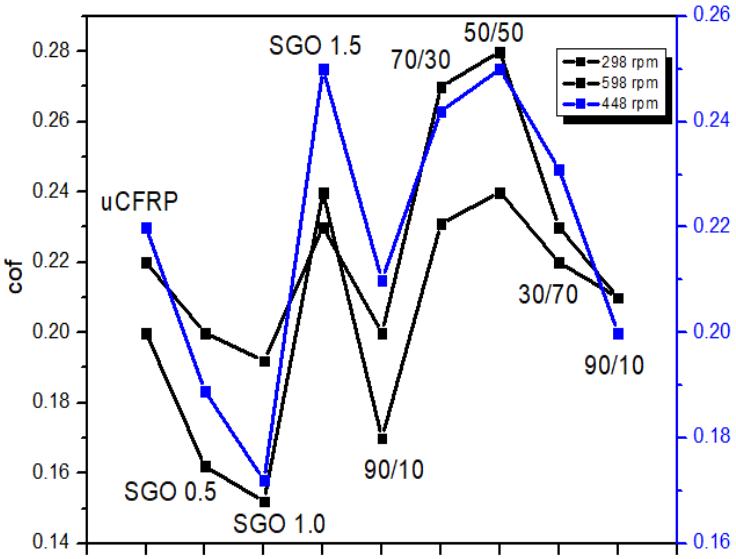

Figure 5.10: Effect of Sliding Velocity characteristics on Coefficient of Friction

In the case of PC/ABS, the decrease in COF as sliding speed increases is a result of ductile shearing and shredding. The ductile shearing and shredding of plastic zones leads to the formation of more resistant zones in the morphology, thereby contributing to a lower C.O.F.

5.1.4.2 Effect of sliding velocity on Wear:

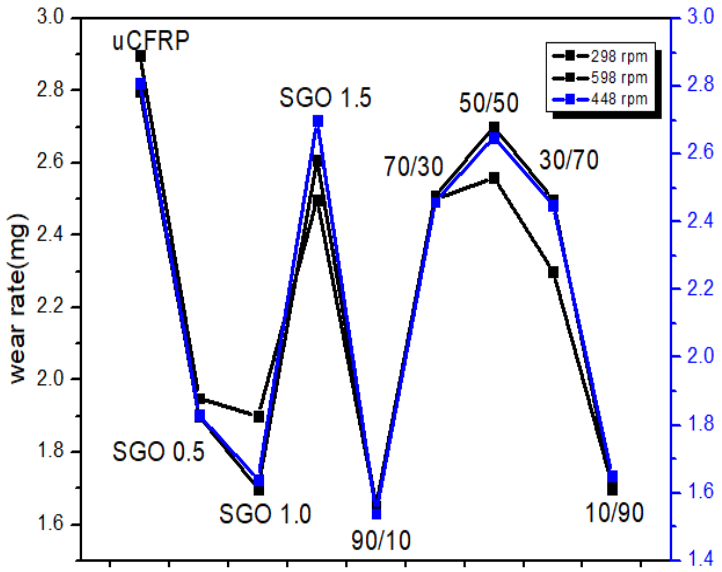

Figure 5.11: CT Effect of Sliding Velocity characteristics on Wear

For cryotreated 5.11, Fig exhibits similar trends to Room Temperature with graphene-coated particles on S.G.O (Graphene Oxide). Graphene particles lubricate contact contacts, reducing friction and wear.Graphene's lubricating characteristics generate an oil film that acts as an interlayer, increasing wear resistance. This interlayer smooths contact surfaces, lowering surface roughness and the risk of asperities causing direct contact erosion. This arrangement absorbs and dissipates sliding energy, minimising heat and wear.

Thus, CFRP with 1.0 S.G.O has the lowest attrition rate. However, when S.G.O concentration exceeds this threshold, oil coatings between contact interfaces tend to rupture, increasing wear rate.

5.2 ANALYSIS OF VARIANCE (ANOVA):

ANOVA is a statistical technique used to determine the significance of each factor on a specific outcome, in this case the coefficient of friction and wear rate (W.R). In order to conduct the ANOVA analysis, the nine sample compositions are separated into distinct groups based on the varying parameter values. The influence of each parameter on the coefficient of friction and wear rate is then independently investigated and analysed.

Using ANOVA, the percentage contribution of each parameter is determined, allowing for a better comprehension of the relative influence of each factor on the outcome. The analysis takes into account the signal-to-noise ratio (S/N) responses '[22], which provide insight into the parameters' effects.

The ANOVA analysis results are presented in a table where the p-values are examined. A decreased p-value indicates that the corresponding parameter exerts a greater influence. To quantify the impact of each parameter, ETA squared, a measure of effect magnitude, is also calculated. The parameters are then ranked based on these results to determine their relative significance.

The general form of ANOVA test for the Sample Test was conducted as follows:

Sample	S.G.O 0.5	S.G.O 1.0	S.G.O 1.5	PC/ABS 10/90	PC/ABS 90/10	PC/ABS 70/30	PC/ABS 30/70	PC/ABS 50/50	Neat
Load	20N		40N		60N		80N		
RPM	298			448			598		

Figure 5.12: ANOVA Table

Table 5.1: ANOVA COF at RT

	df	**sum_sq**	**mean_sq**	**PR(¿F)**	**ETA squared Score**	**Influence**	**Rank**
Sample	8.0	0.090801	0.011350	6.543847e-68	0.7838	Very High Significance	1
Load	1.0	0.001771	0.001771	5.5044e-11	0.01529	moderate	3
RPM	1.0	0.020119	0.0201191	7.2144e-44	0.1736687	High moderate	2
Residual	98.0	0.003157	0.000033	NaN	NaN	NaN	NaN

5.2.1 ANOVA at Room Temperature

5.2.1.1 ANOVA on COF at Room Temperature

As shown in the Table 5.1, the null hypothesis can be rejected for Sample, Load, and RPM based on the P-Value. The exceedingly small P-Value indicates that the sample group's means are significantly affected. Moreover, the squared ETA values provide additional insight into the significance of these factors. where Sample demonstrated a high level of significance while ETA Squared suggested RPM and

Load had a moderate effect.According to the ETA Squared Score, their respective levels of influence on the outcome are indicated ‘[8] ‘[31].

5.2.1.2 ANOVA on wear rate at Room Temperature

Table 5.2: ANOVA Significance C.O.F at RT

	df	**sum_sq**	**mean_sq**	**PR(>F)**	**ETA squared Score**	**Influence**	**Rank**
Sample	8.0	9.864	1.233113	4.873834e-15	-0.53255	Very High Significance	1
Load	1.0	0.025	0.025352	5.641231e-01	-0.0013686	Weak	3
RPM	1.0	1.2906	1.290689	7.711631e-05	-0.069678	moderate	2
Residual	98.0	0.003157	0.000033	NaN	NaN	NaN	NaN

Based on the Table 5.2 ANOVA result, the impact of the wear rate can be determined. The Sample and RPM factors' minuscule p-values indicate that the null hypothesis can be rejected for these factors. This indicates that both Sample and RPM significantly impact the attrition rate. The larger p-value for the Load factor, on the other hand, indicates that there is insufficient evidence to reject the null hypothesis, indicating that Load may not have a significant effect on the wear rate.

Moreover, the squared ETA values provide additional information about the significance of these factors. The Sample factor has a high level of statistical significance, indicating that it has a substantial effect on the attrition rate. The RPM ETA squared value indicates a moderate influence on the attrition rate. As indicated by the Load factor's ETA squared value, the influence of the Load factor is relatively modest.

In conclusion, based on the ANOVA results, the Sample and RPM factors play a significant role in determining the attrition rate, whereas the influence of the Load

factor is less prominent '[8].

5.2.2 ANOVA on C.O.F and Wearrate at Cryo Treated:

5.2.2.1 ANOVA on C.O.F at CryoTreated

Table 5.3: ANOVA Significance C.O.F at CT

	df	**sum_sq**	**mean_sq**	**PR(>F)**	**ETA squared Score**	**Influence**	**Rank**
Sample	8.0	0.063112	0.007889	1.7973e-24	0.5952	Very High Significance	1
Load	1.0	0.013601	0.013601	2.4860e-11	0.12827	High Moderate	2
RPM	1.0	0.006125	0.006125	1.9761e-06	0.057765	moderate	3
Residual	97.0	0.023192	0.000239	NaN	NaN	NaN	NaN

Based on the information as mentioned in the table 5.3, the P-values indicate that the null hypothesis can be rejected for the Sample, Load, and RPM variables. This indicates that these variables have a significant effect on the outcome. A high level of significance is indicated by the Sample factor's extremely low P-value.

In addition, the ETA squared values provide further insight into the significance of these factors. Based on the ETA squared score, the Sample factor demonstrates a high level of significance, indicating that it has a substantial impact on the outcome. On the other hand, the ETA squared values indicate that the Load and RPM factors have a moderate impact.

5.2.2.2 ANOVA on wear rate at Room Temperature

The P-values in the table 5.4 indicate that the null hypothesis can be rejected for the Sample, Load, and RPM variables. This indicates that these variables have a

Table 5.4: ANOVA Significance WearRate at CT

	df	**sum_sq**	**mean_sq**	**PR(>F)**	**ETA squared Score**	**Influence**	**Rank**
Sample	8.0	8.7820	1.0977	1.4541e-11	0.44425	Very High Significance	1
Load	1.0	0.31974	0.31974	6.7349e-02	0.01617	small	3
RPM	1.0	1.60503	1.60503	7.2737e-05	0.0811	moderate	2
Residual	98.0	9.061459	0.093417	NaN	NaN	NaN	NaN

substantial effect on the outcome. The Sample factor's extremely minuscule P-value demonstrates its high level of significance.RPM also displays a reduced P-value, whereas the Load parameter demonstrates some level of significance and requires further investigation.

With the calculated ETA squared values, they provide additional insight into the significance of these factors. Based on the ETA squared score, the Sample factor has a high level of significance, indicating a strong influence on the outcome. However, the ETA squared values indicate a moderate influence for the RPM factor, whereas the load factor has the lowest value, indicating a lesser significance '[8] '[31].

5.3 Taguchi Analysis:

Taguchi analysis is performed to determine the optimal composition under the influencing conditions at room temperature. On the basis of the Pin on Disc experiment, the ANOVA test, and the relative influence of each parameter, the optimal combination of these parameters can be determined using Tagchi analysis.

The pin on disc experiment showed that S.G.O 1.0 and PC/ABS had the lowest wear rate among the compositions, while the analysis of variance test showed that RPM and Load are significant as input parameters to consider.In light of this, a

Taguchi analysis is carried out using the information that follows in order to achieve the most optimal composition at the most optimal parameters.MiniTab is the tool that is used to carry out the action.

5.3.1 Taguchi Analysis-Room Temperature(R.T)

The following table was created using Taguchi optimization with the objective of achieving the desired result (minimal specific wear rate and coefficient of friction) with the fewest number of experiments at Room Temperature. For that L9 Orthogonal Array matrix is created.

Table 5.5: Taguchi Optimized Parameter at RT

Sample	**Load**	**RPM**	**C.O.F**	**Wear**
PC/ABS 90/10	40	298	0.187916	2.6
PC/ABS 90/10	60	448	0.215225	1.6
PC/ABS 90/10	80	598	0.245347	1.5
SGO 1.0	40	448	0.184989	1.78
SGO 1.0	60	598	0.208286	1.7
SGO 1.0	80	298	0.177416	2.31
Neat	40	598	0.263779	2.62
Neat	60	298	0.232	2.6
Neat	80	448	0.260551	2.81

Using Taguchi analysis on the Table 5.5, regression equations describing the relationship between output parameters such as coefficient of friction (COF) and wear rate and input factors such as applied load and rotational speed (RPM) are established. These regression equations assist in quantifying and comprehending the impact of these parameters on the COF.

5.3.1.1 Regression equation Based on Coefficient of friction:

$$C.O.F = 0.1364 + 0.000389Load + 0.000133RPM \tag{5.1}$$

5.3.1.2 Regression equation Based on Coefficient of friction:

$$WearRate = 3.200 - 0.0032Load - 0.00188RPM \tag{5.2}$$

To determine the optimal parameters, the S-N Table is created.The table displays the calculated signal-to-noise ratios used to determine the optimal compositions. These ratios provide information on the performance characteristics under various compositions, allowing us to determine which compositions produce the greatest results.

5.3.1.3 S-N ratio for the C.O.F at Room Temperature:

Table 5.6: C.O.F Signal to Noise Response Table Output

Level	**Sample**	**Load**	**RPM**
1	13.36	13.58	14.08
2	14.43	13.22	13.23
3	11.98	12.97	12.47
Delta	2.45	0.62	1.61
Rank	1	3	2

On the premise of these S-N table 5.6 data , the subsequent result of data is visualized ‘5.13.

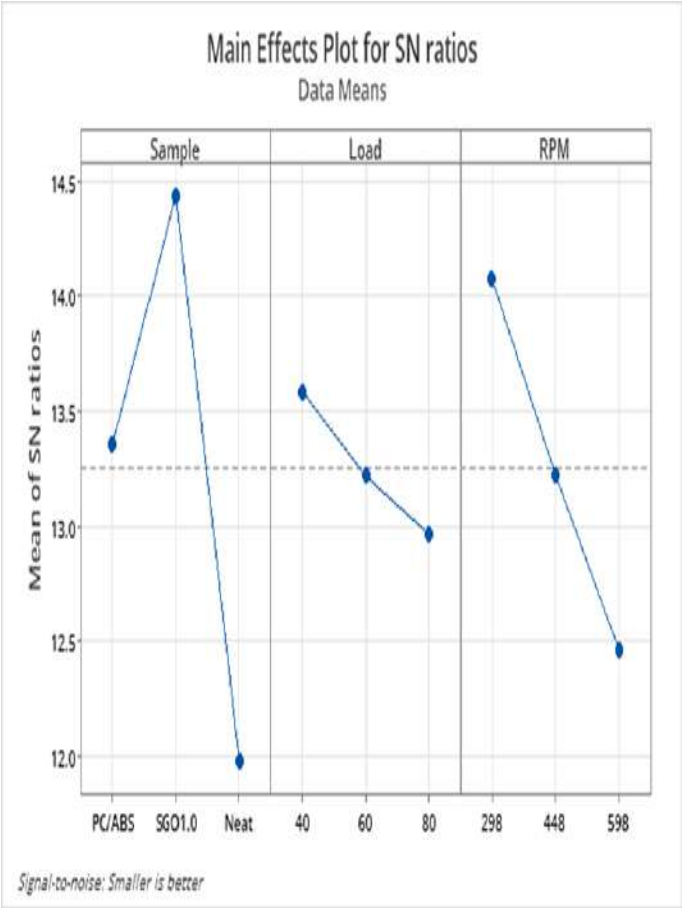

Figure 5.13: S-N Optimized Visualized data

And the best optimum process parameter would be at 5.7

Table 5.7: C.O.F Optimized Result

A2B1C1	**SGO 1.0 40N 298RPM**

5.3.1.4 S-N ratio for the Wear Rate at Room Temperature:

Table 5.8: Wear Rate Signal to Noise Response Table Output

Level	**Sample**	**Load**	**RPM**
1	-5.301	-7.225	-7.957
2	-5.630	-5.664	-6.022
3	-8.547	-6.589	-5.499
Delta	3.245	1.561	2.458
Rank	1	3	2

Based on the above, Level of Significance are in the order Level of significance: **Sample>RPM >Load**

On the premise of these S-N table5.8 data, the subsequent result of data is visualized as shown in fig '5.14.

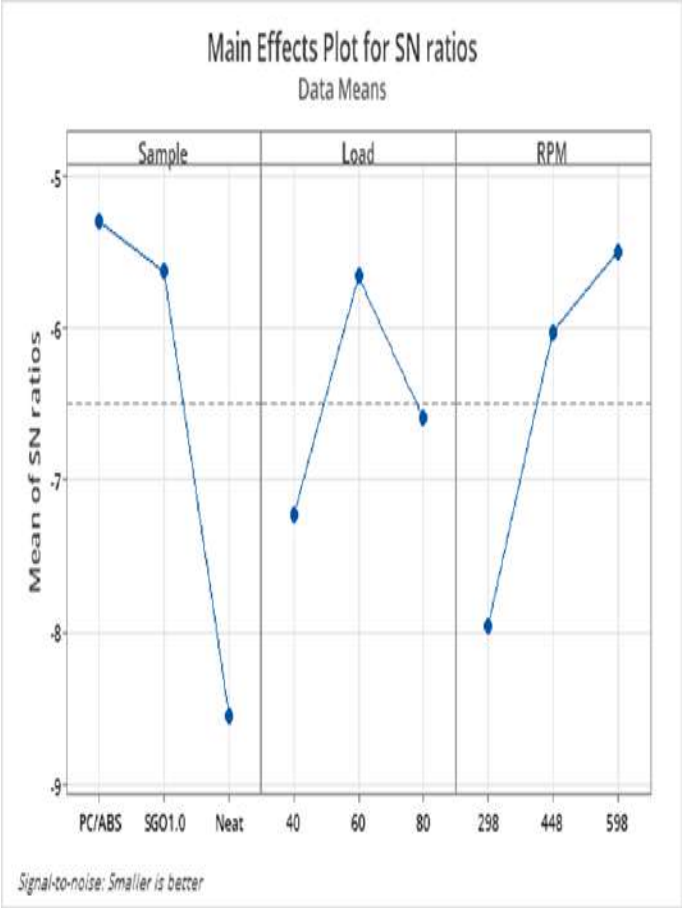

Figure 5.14: S-N Optimized Visualized data

And the best optimum wear rate parameter would be at Table 5.9.

Table 5.9: Optimized wear rate Result

A1B2C3	**PC/ABS 90/10 60N 598RPM**

5.3.2 Taguchi Analysis-Cryo Treated (C.T)

The following table was created using Taguchi optimisation with the objective of achieving the desired result (minimal specific wear rate and coefficient of friction)

with the fewest number of experiments at Cryo Treated condition. For that L9 Orthogonal Array matrix is created.

At Cryo-Treated

Table 5.10: Taguchi Optimized Parameter at CT

Sample	**Load**	**RPM**	**C.O.F**	**Wear**
PC/ABS 90/10	40	298	0.19	2.7
PC/ABS 90/10	60	448	0.23	2.6
PC/ABS 90/10	80	598	0.251	2.61
SGO 1.0	40	448	0.18	2.2
SGO 1.0	60	598	0.200832	2.1
SGO 1.0	80	298	0.19	2.4
Neat	40	598	0.22704	2.53
Neat	60	298	0.26	2.8
Neat	80	448	0.26	2.5

based on the Table 5.10, similar to Room-Temperature condition Using Taguchi analysis, regression equations describing the relationship between output parameters such as coefficient of friction (COF) and wear rate and input factors such as applied load and rotational speed (RPM) are established. These regression equations assist in quantifying and comprehending the impact of these parameters on the COF.

5.3.2.1 Regression equation Based on Coefficient of friction for Cryo-Treated

$$C.O.F = 0.1497 + 0.000866Load + 0.000043RPM \tag{5.3}$$

5.3.2.2 Regression equation Based on Coefficient of friction:

$$WearRate = 2.782 + 0.00067Load - 0.000733RPM \tag{5.4}$$

To determine the optimal parameters, the S-N Table is created.The table displays the calculated signal-to-noise ratios used to determine the optimal compositions. These ratios provide information on the performance characteristics under various compositions, allowing us to determine which compositions produce the greatest results for the Cryo-Treated Condition.

5.3.2.3 S-N ratio for the C.O.F at Cryo-Treated Temperature:

Table 5.11: C.O.F Signal to Noise Response Table Output

Level	**Sample**	**Load**	**RPM**
1	13.07	14.07	13.52
2	14.42	12.80	13.12
3	12.09	12.71	12.94
Delta	2.33	1.36	0.57
Rank	1	2	3

The above Table 5.11 of S-N shows that, for the parameters the significance is in the order

Level of significance: **Sample >Load >RPM**

This is denoted based on the available data, and these tables are then plotted to represent the data.

On the premise of these S-N table data 5.11, the subsequent result of data is visualized as shown in Fig‘5.15.

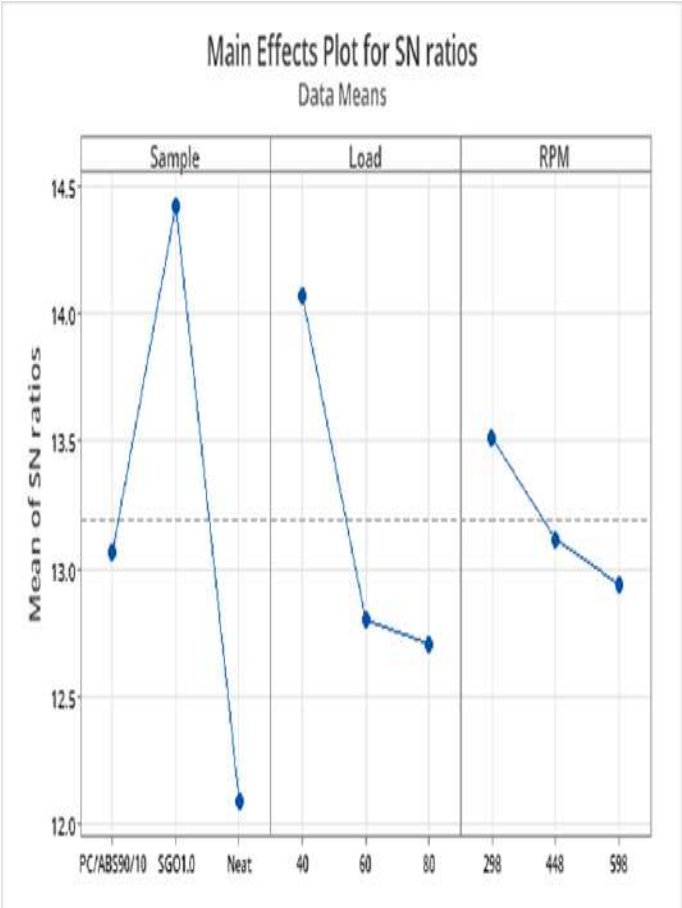

Figure 5.15: S-N Optimized Visualized data

And the best optimum process parameter would be at fig ‘5.12.

Table 5.12: C.O.F Optimized Result

A2B1C1	**SGO 1.0 40N 298RPM**

For the S-N Rate of Cryo Treated-Wear Rate is signified as follows

5.3.2.4 S-N ratio for the Wear Rate at Room Temperature:

The above fig5.13 of S-N shows that, for the parameters the significance is in the order

Level of significance: **Sample >RPM >Load**

On the premise of these S-N table data, the subsequent result of data is visualized as shown in fig ‘5.16.

Table 5.13: Wear Rate Signal to Noise Response Table Output

Level	**Sample**	**Load**	**RPM**
1	-8.420	-7.846	-8.392
2	-6.966	-7.896	-7.702
3	-8.321	-7.965	-7.613
Delta	1.454	0.119	0.778
Rank	1	3	2

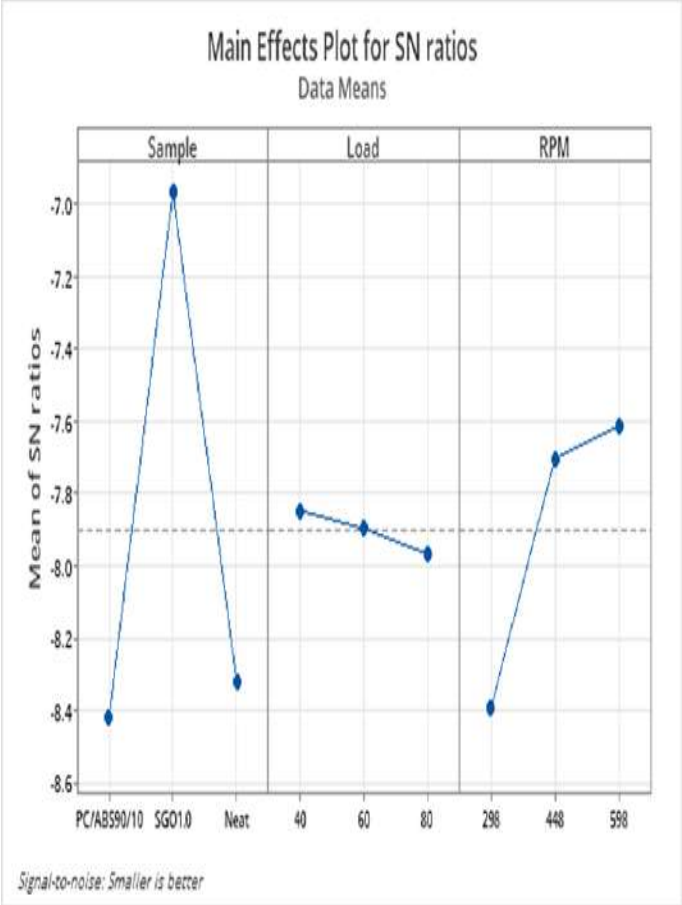

Figure 5.16: S-N Optimized Visualized data

And the best optimum wear rate parameter at Cryo-treated condition would be at fig ‘5.14,

Table 5.14: Optimized wear rate Result

A2B1C3	**S.G.O 1.0 40N 598RPM**

An analysis of variance (ANOVA) is the next step that needs to be taken in order to do additional validation of the conformity of significance RPM and Load have

with the output parameter on the MiniTab Softaware. The purpose of this study is to investigate the effect that RPM and Load have on the qualities exhibited by both RT and CT.

5.4 ANOVA and its significance on RPM and Load

$$S/N = -10 \log \left(\frac{1}{n} \sum_{i=1}^{n} y^2 \right) \tag{5.5}$$

Based on Equation 5.5, on the condition smaller is better

5.4.1 ANOVA S-N ratio on C.O.F and wear at Room Temperature

5.4.1.1 ANOVA for C.O.F

Table 5.15: ANOVA for Significance of Load and RPM on C.O.F at RT

Source	df	Adj SS	Adj MS	P-Value
Regression	2	0.002766	0.001383	0.311
Load	1	0.002403	0.000362	0.563
RPM	1	0.002766	0.002403	0.166
Error	6	0.005809	0.000968	NaN
Total	8	0.008574	NaN	NaN

on the fig ‘5.15,When compared to the Load parameter, the RPM parameter has a smaller value, which indicates that it is of more significance. This can be seen by referring to the table that has been provided. This outcome is consistent with the findings gained from prior experiments and statistical testing, which provides additional evidence that its influence is real.

5.4.1.2 ANOVA for Wear Rate(Smaller is Better)

On the fig ‘5.16, When it comes to the effect of wear, RPM over Load has the most significant influence, which was the pattern that was followed before and was in accordance with the test.

Table 5.16: ANOVA for Significance of Load and RPM on WearRate at RT

Source	df	Adj SS	Adj MS	P-Value
Regression	2	0.50008	0.25004	0.452
Load	1	0.02407	0.02407	0.777
RPM	1	0.47602	0.47602	0.236
Error	6	1.64821	0.2747	NaN
Total	8	2.14829	NaN	NaN

5.4.2 ANOVA S-N ratio on C.O.F and wear at Cryo-Treated

5.4.2.1 ANOVA for C.O.F

Table 5.17: ANOVA for Significance of Load and RPM on C.O.F at CT

Source	df	Adj SS	Adj MS	P-Value
Regression	2	0.002053	0.001027	0.414
Load	1	0.001801	0.001801	0.229
RPM	1	0.000252	0.000252	0.634
Error	6	0.006016	0.001003	NaN
Total	8	0.008069	NaN	NaN

As shown in fig ‘5.17,When compared to the RPM parameter, the load parameter has a smaller value, which indicates that the load parameter is more significant. This can be seen by referring to the table that has been provided. This outcome is consistent with the findings gained from prior experiments and statistical testing, which provides additional evidence that its influence is real.

5.4.2.2 ANOVA for Wear Rate

Smaller is Better

For the Table ‘5.18, the effect of wear, RPM over Load has the most significant influence, which was the pattern that was followed before and was in accordance with the test.

Table 5.18: ANOVA for Significance of Load and RPM on WearRate at CT

Source	**df**	**Adj SS**	**Adj MS**	**P-Value**
Regression	2	0.073667	0.036833	0.554
Load	1	0.001067	0.001067	0.895
RPM	1	0.072600	0.072600	0.300
Error	6	0.338933	0.056489	NaN
Total	8	0.412600	NaN	NaN

5.5 Machine Learning and Artificial Neural Network:

The practise of employing neural networks and machine learning as a form of computational tool and how it can establish a complex non-linear relationship was gleaned from various journals and references. In the past, these techniques were used to predict the mechanical properties of various materials and optimise the microstructures of materials.Due to the incorporation of Machine Learning and Artificial Intelligence (AI), we are able to accurately predict the tribological properties of CFRP materials using this method. Consequently, we are able to comprehend the data's underlying patterns and correlations, which in this instance were the wear and Coefficient of Friction. After training, they can be used to make predictions about the tribological behaviour under new input conditions, which can provide extremely valuable insights for design and optimisation purposes.

Following the conclusion of the necessary preliminary procedures, which included data cleansing, preprocessing, and the division of the dataset, we analysed the data using a variety of machine learning models. Each model was trained using the training data, and its performance was then evaluated using the most relevant metrics available.

The evaluation metrics, including mean squared error (MSE) and R-squared, were used to determine how accurately each model predicted the tribological behaviour of CFRP. These insights have been utilised to enhance the models. The model with the highest R-squared value or the lowest error was determined to be the most accurate for making predictions.

Because we select the model with the smallest quantity of error, we anticipate that it will generate more accurate predictions and have superior generalisation performance. This model has demonstrated that it is capable of capturing the underlying patterns and relationships in the data; as a result, it can be used to predict the tribological behaviour of CFRP.

In order to produce accurate predictions and gain useful insights into the tribological properties of CFRP (Carbon Fibre Reinforced Polymer), it is necessary to select the model that performs the best based on its characteristics. By accurately estimating the wear and friction properties of the material, we can maximise the effectiveness of CFRP in a variety of applications.

On the basis of the journal, we are able to compare the performance of various predictive models, such as Linear Regression, Neural Network, and the Levenberg-Marquardt Algorithm, and select the model that best meets our specific needs by selecting the model with the best overall performance. We can determine which model produces the most accurate predictions by comparing the results of the various models, each of which has its own strengths and weaknesses.

Then, a comparative analysis is conducted, which enables us to comprehend the advantages and disadvantages of each model so that we can select the one that best meets our specific needs. This method enhances our knowledge of the tribological properties of CFRP and enables more effective decision-making regarding the optimal use of CFRP in a variety of applications.

Utilising techniques such as machine learning and predictive modelling will allow us to gain a deeper understanding of the behaviour of CFRP and make more informed decisions regarding the application of this material. This ultimately results in enhanced performance, dependability, and efficiency in industries that utilise CFRP materials.

5.5.1 At Room Temperature

Table 5.19: Optimized wear rate Result

Sl.No	ML Models	Mean Square Error(MSE)
1	**Linear Regression(LR)**	**4.9%**
2	**Neural network(N.N)**	**3%**
3	**Levenberg Marquardt**	**0.35%**

5.5.2 At Cryo-Treated Condition

Table 5.20: Optimized wear rate Result

Sl.No	ML Models	Mean Square Error(MSE)
1	**Linear Regression(LR)**	**5.75%**
2	**Neural network(N.N)**	**5%**
3	**Levenberg Marquardt**	**0.88%**

On the basis of the table 5.19 , 5.20 , the Levenberg-Marquardt algorithm displayed the optimum performance. In comparison to the other models, it had MSE values that were lower for both the Room Temperature and the Cryo-Treated conditions. A lower MSE implies that the Levenberg-Marquardt algorithm's predictions were closer to the actual values, indicating a better level of accuracy. This is indicated by the fact that the MSE is lower.

Thus, Levenberg-Marquardt algorithm is then visualized showing that
At RT:

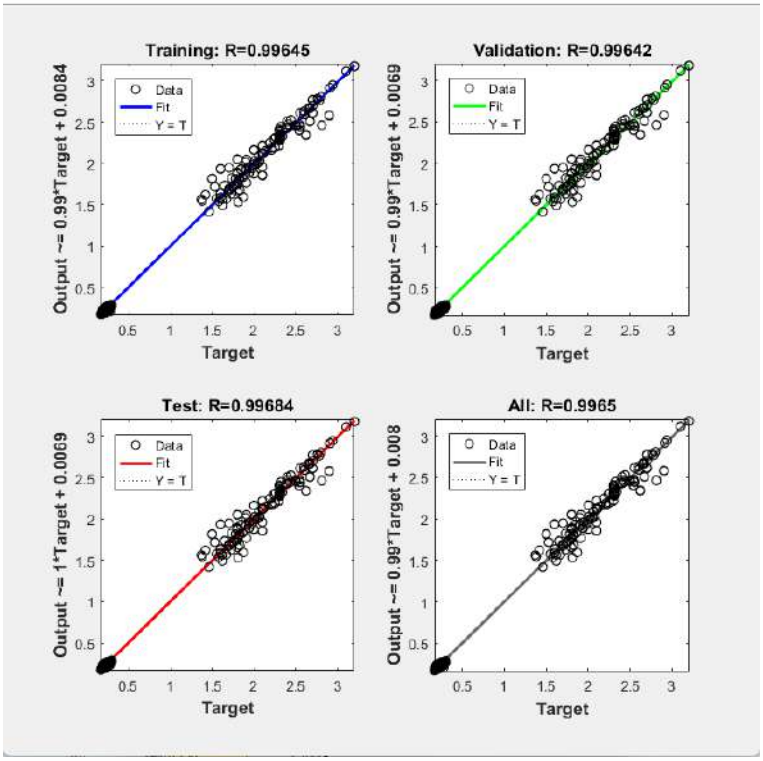

Figure 5.17: RT Actual V/s Predicted

At CT:

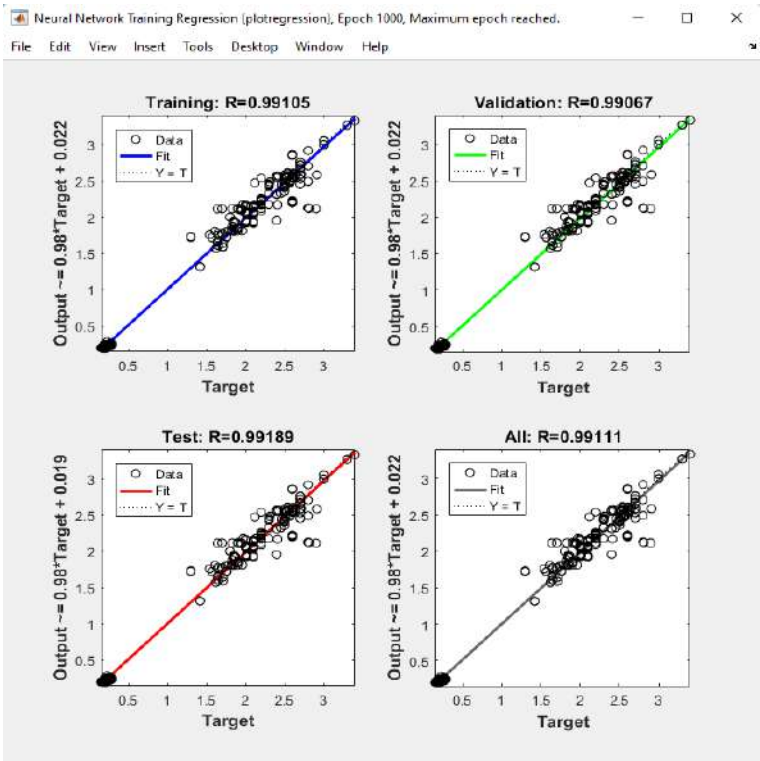

Figure 5.18: RT Actual V/s Predicted

Based on the Fig 5.17 and Fig ‘5.18,The comparison between predicted and actual values of the provided data reveals that the Levenberg model exhibits a

higher level of accuracy and proximity in its predicted values compared to other models. This suggests that the Levenberg model is more effective in capturing the underlying patterns and trends in the data, leading to more reliable predictions. The observed closeness between the predicted and actual values indicates the superior performance of the Levenberg model in this specific analysis.

The improved performance of the Levenberg-Marquardt algorithm shows that it is better suited for forecasting the tribological behaviour of CFRP under both Room Temperature and Cryo-Treated circumstances. This conclusion is based on the fact that the method has performed exceptionally well in previous applications. It is possible for it to produce more trustworthy and accurate forecasts, which are essential for comprehending the functionality and behaviour of CFRP materials in a variety of situations.

predicted values V/s actual values are:

AT Room Temperature:

A	B	C	D	E	F	G	H	I	J
Time serie	Sample	Sample	Load	RPM	COF	Wear	LevenBErg_COF_pred	LevenBErg_wear_predicted	
1	50-50	2	20	298	0.256	2.7	0.259805471	2.708676555	
2	50-50	2	20	298	0.256	2.7	0.259814761	2.708634062	
3	50-50	2	20	298	0.256	2.7	0.259824052	2.708591593	
4	50-50	2	20	298	0.256	2.7	0.259833343	2.708549148	
5	50-50	2	20	298	0.256	2.7	0.259842634	2.708506729	
6	50-50	2	20	298	0.256	2.7	0.259851926	2.708464334	
7	50-50	2	20	298	0.256	2.7	0.259861217	2.708421964	
8	50-50	2	20	298	0.256	2.7	0.259870509	2.708379619	
9	50-50	2	20	298	0.256	2.7	0.259879802	2.708337299	
10	50-50	2	20	298	0.256	2.7	0.259889095	2.708295004	
11	50-50	2	20	298	0.256	2.7	0.259898388	2.708252734	
12	50-50	2	20	298	0.256	2.7	0.259907681	2.708210489	
13	50-50	2	20	298	0.256	2.7	0.259916975	2.70816827	
14	50-50	2	20	298	0.256	2.7	0.259926269	2.708126075	
15	50-50	2	20	298	0.256	2.7	0.259935563	2.708083905	
16	50-50	2	20	298	0.256	2.7	0.259944857	2.708041761	
17	50-50	2	20	298	0.256	2.7	0.259954152	2.707999642	
18	50-50	2	20	298	0.256	2.7	0.259963447	2.707957548	
19	50-50	2	20	298	0.256	2.7	0.259972743	2.707915479	
20	50-50	2	20	298	0.256	2.7	0.259982038	2.707873436	
21	50-50	2	20	298	0.256	2.7	0.259991334	2.707831418	
22	50-50	2	20	298	0.256	2.7	0.260000631	2.707789425	
23	50-50	2	20	298	0.256	2.7	0.260009927	2.707747458	
24	50-50	2	20	298	0.256	2.7	0.260019224	2.707705517	
25	50-50	2	20	298	0.256	2.7	0.260028521	2.707663601	
26	50-50	2	20	298	0.256	2.7	0.260037819	2.70762171	
27	50-50	2	20	298	0.256	2.7	0.260047116	2.707579846	
28	50-50	2	20	298	0.256	2.7	0.260056414	2.707538006	
29	50-50	2	20	298	0.256	2.7	0.260065713	2.707496193	
30	50-50	2	20	298	0.256	2.7	0.260075011	2.707454405	
31	50-50	2	20	298	0.256	2.7	0.26008431	2.707412643	
32	50-50	2	20	298	0.256	2.7	0.260093609	2.707370907	
33	50-50	2	20	298	0.256	2.7	0.260102908	2.707329196	
34	50-50	2	20	298	0.256	2.7	0.260112208	2.707287512	
35	50-50	2	20	298	0.256	2.7	0.260121508	2.707245853	
36	50-50	2	20	298	0.256	2.7	0.260130808	2.70720422	
37	50-50	2	20	298	0.256	2.7	0.260140108	2.707162613	
38	50-50	2	20	298	0.256	2.7	0.260149409	2.707121033	

Figure 5.19: RT Actual V/s Predicted

At Cryo-Treated condition:

A	B	C	D	E	F	G	H	I	J	K	L	M
Time serie	Sample	Sample	Load	RPM	COF	Wear	LR_COF	LR_wear	NN_COF Predicte	NN_Wear pred	LM_COF	LM_Wear
1	50-50	2	20	298	0.24	2.7	0.21360964	2.139589554	0.232431471	2.111938	0.23824722	2.679476464
2	50-50	2	20	298	0.24	2.7	0.21362308	2.139605331	0.231860101	2.111297607	0.23824723	2.679446128
3	50-50	2	20	298	0.24	2.7	0.21363651	2.139621108	0.231560856	2.11053896	0.23824723	2.679415792
4	50-50	2	20	298	0.24	2.7	0.21364994	2.139636884	0.231388271	2.109506607	0.23824724	2.679385457
5	50-50	2	20	298	0.24	2.7	0.21366337	2.139652661	0.231195346	2.108375549	0.23824724	2.679355121
6	50-50	2	20	298	0.24	2.7	0.21367681	2.139668438	0.23100245	2.107244492	0.23824724	2.679324786
7	50-50	2	20	298	0.24	2.7	0.21369024	2.139684215	0.230809644	2.106113434	0.23824725	2.67929445
8	50-50	2	20	298	0.24	2.7	0.21370367	2.139699992	0.230616763	2.104982376	0.23824725	2.679264115
9	50-50	2	20	298	0.24	2.7	0.21371711	2.139715769	0.230423838	2.103850842	0.23824725	2.67923378
10	50-50	2	20	298	0.24	2.7	0.21373054	2.139731546	0.230231002	2.102720022	0.23824726	2.679203444
11	50-50	2	20	298	0.24	2.7	0.21374397	2.139747323	0.230069786	2.102310896	0.23824726	2.679173109
12	50-50	2	20	298	0.24	2.7	0.2137574	2.1397631	0.229917884	2.102116823	0.23824727	2.679142774
13	50-50	2	20	298	0.24	2.7	0.21377084	2.139778877	0.229766041	2.10192275	0.23824727	2.679112439
14	50-50	2	20	298	0.24	2.7	0.21378427	2.139794654	0.229614258	2.101728439	0.23824727	2.679082104
15	50-50	2	20	298	0.24	2.7	0.2137977	2.139810431	0.229462415	2.101534605	0.23824728	2.679051769
16	50-50	2	20	298	0.24	2.7	0.21381114	2.139826208	0.229310244	2.101356983	0.23824728	2.679021434
17	50-50	2	20	298	0.24	2.7	0.21382457	2.139841985	0.229120508	2.102748156	0.23824728	2.678991099
18	50-50	2	20	298	0.24	2.7	0.213838	2.139857762	0.228930876	2.104139328	0.23824729	2.678960764
19	50-50	2	20	298	0.24	2.7	0.21385143	2.139873539	0.228741303	2.1055305	0.23824729	2.67893043
20	50-50	2	20	298	0.24	2.7	0.21386487	2.139889315	0.228551656	2.106921673	0.23824729	2.678900095
21	50-50	2	20	298	0.24	2.7	0.2138783	2.139905092	0.228361994	2.108312607	0.2382473	2.67886976
22	50-50	2	20	298	0.24	2.7	0.21389173	2.139920869	0.228172332	2.109704018	0.2382473	2.678839426

Figure 5.20: CT Actual V/s Predicted

5.6 Microscopic Sample Analysis

The samples that have given the best performance at very high speed of 598 RPM and 80N are then gold cotted and are analysed using an optical metallurgical Microscope. We can see that for the S.G.O samples in the figure ‘5.21,‘5.22, due to the agglomeration effect, the Si-O-Si being forming a thin layer on the surface of the sample, which has reduced the Coefficient of friction.Similarly, for the PC/ABS observed from the reference figure ”PC/ABS 90/10 Gold Cotted,” the ABS was shown to develop particle morphology within the PC, and these synergestic particles were seen to become elongated as a result of contact load pressure and extremely high speed.

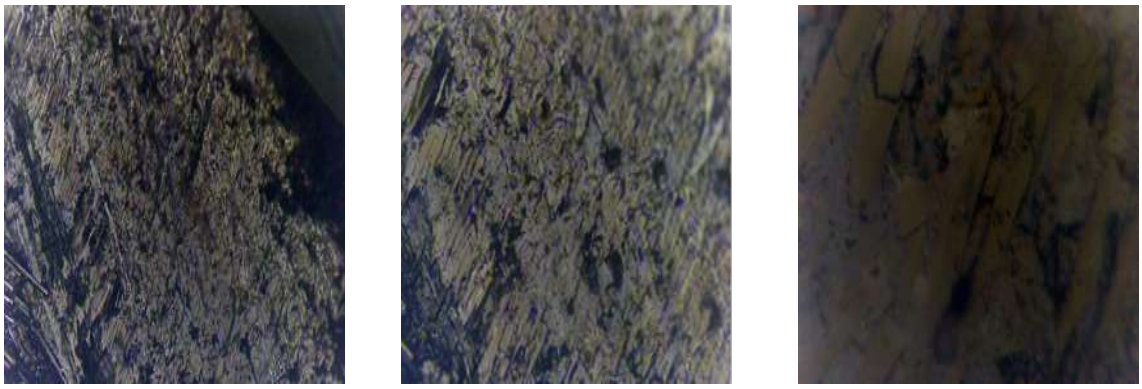

(a) 100X (b) 200X (c) 1000X

Figure 5.21: S.G.O 1.0

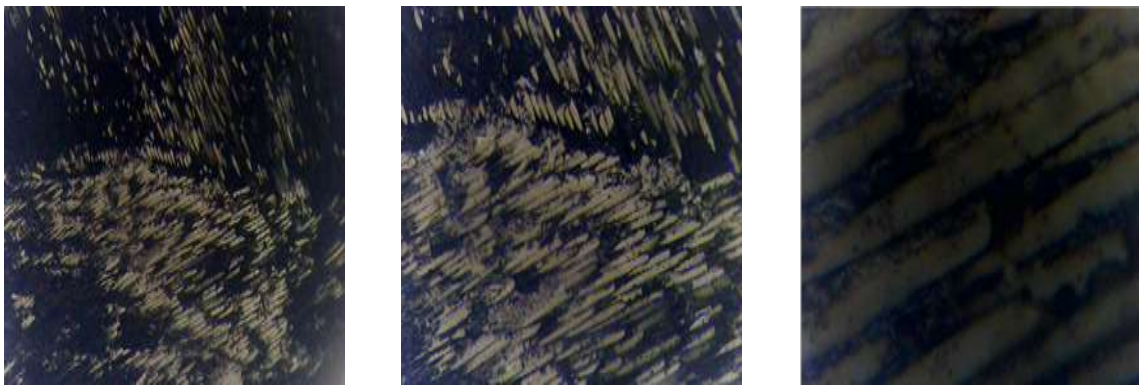

(a) 100X (b) 200X (c) 1000X

Figure 5.22: PC/ABS

Chapter 6

CONCLUSION

The effects of force and sliding velocity are investigated under a variety of tribological situations, in various combinations of different compositions, for both room temperature and cryo-treated materials.

For S.G.O on both the coefficient of friction (COF) and the wear rate (WR), for which SGO1.0 decreased, showing the lubricating behaviour of GO particles and the involvement of Si-O-Si bonds in lowering WR.

A lower coefficient of friction was observed in the PC/ABS blend when either PC or ABS was present in higher proportions. However, both COF and WR increased as the range moved towards the middle.

Because of the increased brittle behaviour in the Cryo-Treated Condition, the COF and WR increased with increasing load and sliding speed. This was caused by the cryogenic treatment.

Both the Taguchi and the ANOVA analyses came to the conclusion that Sample composition, Load, and RPM are significant parameters that influence production. Load had comparatively less importance than sample composition and RPM due to adhesion effects during sliding velocity. Sample composition showed the highest level of relevance, followed by RPM.

Both the Taguchi analysis and the ANOVA analysis produced similar findings, which served as validation during the testing process.

Three models, one of which was the Levenberg Marquardt Algorithm (CT), were implemented with low mean squared error (MSE) values; the RT value was 0.35%, and the CT value was 0.88%.

Examination of the gold-coated samples using a metallurgical microscope provided additional confirmation of the identified tendencies.

By analyzing the wear behavior, we can now optimize the performance and select

CFRP compositions that can withstand the more demanding conditions in aerospace environments.

This improves the chances of selecting CFRP as an alternative, as these experiments can now help in modifying the CFRP components which is giving minimum wear, and improve load distribution. Thus improving maintenance and reliability, ultimately reducing downtime and improving overall efficiency.

REFERENCES

[1] **Kareem S Aggour, Vipul K Gupta, Daniel Ruscitto, Leonardo Ajdelsztajn, Xiao Bian, Kristen H Brosnan, Natarajan Chennimalai Kumar, Voramon Dheeradhada, Timothy Hanlon, Naresh Iyer, et al.(** 2019) Artificial intelligence/machine learning in manufacturing and inspection: A ge perspective. MRS Bulletin, 44(7):545–558.

[2] **Huda A Al-Salihi, Adil Akram Mahmood, and Hussain J Alalkawi**.(2019), Mechanical and wear behavior of aa7075 aluminum matrix composites reinforced by al2o3 nanoparticles. Nanocomposites, 5(3):67–73.

[3] **J Aravind, M Manu, KE Reby Roy, M Mubarak Ali, Shukur Bin Abu Hassan, S Rajalekshmi, and Desin S Daniel**,(2023), Thermal synergistic effect on cfrp laminates with modified fiber/matrix systems for heat transfer applications. Macromolecular Chemistry and Physics, 224(11):2200462.

[4] **Anay Arun and Kalyan Kumar Singh.(** 2017) Friction and wear behavior of glass fibre reinforced polymer composite (gfrp) under dry and oil lubricated environmental conditions. Materials Today: Proceedings, 4(8):7285–7292.

[5] Pooja Bhatt and Alka Goe. Carbon fibers: production, properties and potential use. Mater. Sci. Res. India, 14(1):52–57, 2017.

[6] **A Borjali, K Monson, and B Raeymaekers.(** 2019) Predicting the polyethylene wear rate in pin-on-disc experiments in the context of prosthetic hip implants: Deriving a data-driven model using machine learning methods. Tribology international, 133:101–110.

[7] **J Paulo Davim and Pedro Reis**. (2003) Study of delamination in drilling carbon fiber reinforced plastics (CFRP) using design experiments. Composite structures, 59(4):481–487.

[8] **Wutao Dong, Songlin Nie, and Anqing Zhang**. (2013),Tribological behavior of peek filled with cf/ptfe/graphite sliding against stainless steel surface under water lubrication. Proceedings of the Institution of Mechanical Engineers, Part J: Journal of Engineering Tribology, 227(10):1129–1137.

[9**] Henri P Gavin**.(2019). The Levenberg-Marquardt algorithm for nonlinear least squares curve-fitting problems. Department of civil and environmental engineering, Duke University, 19.

[10] **Milan V Gordi´c, IM Djordjevi´c, Danijela R Sekuli´c, ZS Petrovi´c, and MM Stevanovi´c**. (2007). Delamination strain energy release rate in carbon fiber/epoxy resin composites. In Materials Science Forum, volume 555, pages 515–519. Trans Tech Publ.

[11] **Yu-xin He, Qi Li, Tapas Kuila, Nam Hoon Kim, Tongwu Jiang, Kin-tak Lau, and Joong Hee Lee**. (2013) Micro-crack behavior of carbon fiber reinforced thermoplastic modified epoxy composites for cryogenic applications. Composites Part B: Engineering, 44(1):533–539.

[12] **Hamid Khayyam, Reza N Jazar, Srinivas Nunna, Gelayol Golkarnarenji, Khashayar Badii, Seyed Mousa Fakhrhoseini, Satish Kumar, and Minoo Naebe,** (2020) Pan precursor fabrication, applications and thermal stabilization process in carbon fiber production: Experimental and mathematical modelling. Progress in Materials Science, 107:100575.

[13] **Santosh Kumar, Nikhil Sharma, and KK Singh**,(2023) Artificial neural network technique to assess tribological performance of gfrp composites incorporated with graphene nano-platelets. Tribology International, 179:108–194.

[14**] Halil Ibrahim Kurt, Murat Oduncuoglu, et al**, (2015), Application of a neural network model for prediction of wear properties of ultrahigh molecular weight polyethylene composites. International Journal of Polymer Science.

[15] **Wuzhou Li, Liangang Zheng, Yang Gao, Yuzhe Xie, and Fujun Xu**, (2021) Interfacial bonding enhancement between cryogenic conditioned carbon fiber and epoxy resin characterized by the single-fiber fragmentation method. AATCC Journal of Research, 8(4):1–7.

[16] **Yan Li, Han Zhang, Yi Liu, Huasheng Wang, Zhaohui Huang, Ton Peijs, and Emiliano Bilotti,** (2018), Synergistic effects of spray-coated hybrid carbon nanoparticles for enhanced electrical and thermal surface conductivity of cfrp laminates. Composites Part A: Applied Science and Manufacturing, 105:9–18.

[17] **M Manu, KE Reby Roy, M Mubarak Ali, and Austin A Mathew**,(2022), Experimental study on silane as an epoxy additive for improving the impact strength of cfrp composites at cryogenic temperatures. Materials Today: Proceedings, 52:2279–2284.

[18] **M Manu, KE Reby Roy, Shukur Bin Abu Hassan, Akhil Masihadas, et al**, (2022) Effect of epd coated silanized graphene oxide on carbon fiber reinforced plastic: An emphasis on mechanical properties at cryogenic temperatures. Surface and Coatings Technology, 451:129043.

[19] **Sayed Abolfazl Mirdehghan,(** 2021) Fibrous polymeric composites. In Engineered Polymeric Fibrous Materials, pages 1–58. Elsevier.

[20] **Challa Gangu Naidu, Challa VV Ramana, Yarraguntla Srinivasa Rao, Kollabathula Vara Prasada Rao, Dadi Vasudha, Gandi Anusha, and Koppisetty B Rajeshbabu**, (2023),A concise review on carbon fiber-reinforced polymer (cfrp) and their mechanical significance including industrial applications. Carbon Nanotubes-Recent Advances, New Perspectives and Potential Applications.

[21] **Klaudia Olejniczak and Jerzy Napi´orkowski**. (2022) Abrasive wear resistance of matrix

composites carbon fiber reinforced polymers. Technical Sciences/University of

Warmia and Mazury in Olsztyn, (25 (1).

[22] **N Ozsoy, M Ozsoy, and A Mimaroglu**.(2017), Taguchi approach to tribological behaviour of chopped carbon fiber-reinforced epoxy composite materials. Acta

Physica Polonica A, 132(3):846–848.

[23] **K Palanikumar**, (2012), Analyzing surface quality in machined composites. In Machining technology for composite materials, pages 154–182. Elsevier.

[24] **Hiral H Parikh and Piyush P Gohil.** (2017) Experimental investigation and prediction

of wear behavior of cotton fiber polyester composites. Friction, 5:183–193.

[25] **Prabhat Kumar Prajapati, Santosh Kumar, and KK Singh,** (2020), Optimization of tribological behavior of cfrp composites under dry sliding condition using taguchi

method. Materials Today: Proceedings, 21:1320–1329.

[26] **Wei Shao, Quanxing Sun, Xu Xu, Wenhan Yue, and Danda Shi**,(2023), Durability

life prediction and horizontal bearing characteristics of cfrp composite piles in

marine environments. Construction and Building Materials, 367:130116.

[27] **Vipin Kumar Tripathi and Shailesh Ambekar**,(2019), Optimization and analysis of

wear rate of cfrp-nanozno/nanoclay hybrid composites using rsm. Journal of

Bio-and Tribo-Corrosion, 5:1–13.

[28] **Jinhua Wei, Bin Lin, Haoji Wang, Tianyi Sui, Shuai Yan, Feifei Zhao, Anying**

Wang, and Sheng Fang,(2018), Friction and wear characteristics of carbon fiber reinforced silicon carbide ceramic matrix (cf/sic) composite and zirconia (zro2)

ceramic under dry condition. Tribology International, 119:45–54.

[29] **Chang-Mou Wu, Yi-Ching Cheng, Wen-You Lai, Po-Hsun Chen, and TzongDer Way**,(2020), Friction and wear performance of staple carbon fabric-reinforced

composites: Effects of surface topography. Polymers, 12(1):141,.

[30] **Xianbo Xu and Nikhil Gupta,** (2019), Artificial neural network approach to determine

elastic modulus of carbon fiber-reinforced laminates. Jom, 71(11):4015–4023.

[31] **Zhenhua Zhang, Songlin Nie, Wuju Liao, Lei Li, and Shaohua Yuan**,(2014), Tribological behaviors of carbon fiber reinforced polyetheretherketone sliding against silicon carbide ceramic under seawater lubrication. Proceedings of the Institution of

Mechanical Engineers, Part J: Journal of Engineering Tribology, 228(12):1421–

1432.

LIST OF PUBLICATIONS

1. **K E Reby Roy, Aravind J, Manu M, Mubarak Ali M, Ajimshad A, Mohammed Sanal B,(2023)** A comparative investigation of the effects of EPD-modified and plastic-modified CFRPs from the perspective of wear characteristics-Materials Letters(Under Review)